Renewable and Sustainable Energy Reviews 92 (2018) 658–675

Contents lists available at ScienceDirect

Renewable and Sustainable Energy Reviews

journal homepage: www.elsevier.com/locate/rser

A comprehensive review on heat transfer and pressure drop characteristics and correlations with supercritical CO_2 under heating and cooling applications

M. Monjurul Ehsan*, Zhiqiang Guan, A.Y. Klimenko

The Queensland Geothermal Energy Centre of Excellence (QGECE), School of Mechanical and Mining Engineering, The University of Queensland, Brisbane, QLD 4072, Australia

ARTICLE INFO

Keywords:
Supercritical CO_2
Heat transfer
Pressure drop
Buoyancy
Correlation

ABSTRACT

The CO_2 with superior thermo-physical properties has numerous applications in nuclear reactor, power plant, refrigeration and air conditioning systems as well as in many engineering and industrial applications. The complex phenomenon of thermal and hydrodynamic behaviour associated with supercritical CO_2 is a continuing research topic for many researchers. The conventional correlations of turbulent forced convection heat transfer failed to predict the heat transfer and flow behaviour especially in the vicinity of the critical condition. The present paper presents a comprehensive review of heat transfer characteristics and correlations with supercritical CO_2 employed under heating and cooling condition in horizontal channel or tube. An exhaustive review of implementation of supercritical CO_2 used with horizontal and vertical orientation of tubes under turbulent flow condition and other operating parameters (inlet sCO_2 pressure, mass flux, temperature, and heat flux) is also reported. In the present work, possible reasons for heat transfer deterioration under heating of supercritical CO_2 are discussed. The characteristics of pressure drop, convective heat transfer behaviour, effect of buoyancy, the wall temperature distribution and finally the comparison among different correlations are reviewed extensively for supercritical CO_2. The study of these correlations with their range of applicability provides a good insight for efficient thermal design and optimization of heat exchanger especially in thermal power plants.

1. Introduction

The conventional CFC (chlorofluorocarbon) and HCFC (hydrochlorofluorocarbon) refrigerants due to their environmental hazards such as global warming and ozone depletion are now being gradually phased out. The refrigeration technology finds their numerous application in food storage, chemical and process industries as well as in other engineering and industrial applications [1]. However, the leakage and serious global warming associated with the traditional refrigerants, the refrigerant industries and researchers investigated for a safe refrigerant substitute to subside the green house problem. The fluorocarbon chemical industries have offered chloride free HFC refrigerants for efficient design of heat pumps and heat exchanger but still they offer considerable global warming impact. A substantial number of experimental and theoretical investigations have been reported for identification and development of a chloride free natural refrigerant substitute [2–5]. The possible environmentally benign refrigerant candidates were water [6], helium [7,8], hydrogen [9], ammonia [10] and carbon dioxide. Among all these refrigerant substitutes, CO_2 with zero ozone depletion potential has been employed as a heat transfer fluid in conventional refrigeration and air conditioning system. Due to its superior physical and transport properties, CO_2 refrigeration system have extensive implementation in automotive air conditioning, commercial and residential air conditioning, and various industrial uses [11,12]. CO_2, a nontoxic, non-flammable natural fluid, provides full personal and environmental safety and economic operation. The attractive thermodynamic and physical properties like specific heat at constant pressure and lower specific volume make CO_2 as one of the best refrigerant substitutes in comparison with conventional refrigerants.

In traditional refrigeration and air conditioning system, both heat rejection and heat absorption take place under subcritical pressure and temperature. In conventional refrigeration cycle, the refrigerant changes its state from vapour to liquid by a condensation process in a high-pressure heat exchanger known as condenser. The critical temperature (31.1 °C) and pressure (7.38 MPa) of CO_2 enable the refrigeration system to work under a trans-critical cycle. In CO_2 refrigeration system, the isobaric heat absorption operates under subcritical condition whereas the heat rejection takes place under

* Corresponding author.
E-mail addresses: m.ehsan@uqconnect.edu.au (M.M. Ehsan), guan@uq.edu.au (Z. Guan), a.klimenko@uq.edu.au (A.Y. Klimenko).

https://doi.org/10.1016/j.rser.2018.04.106
Received 27 November 2017; Received in revised form 26 March 2018; Accepted 21 April 2018
Available online 10 May 2018

Nomenclature

A	area, m^2
C_p	specific heat at constant pressure, J/kg K
D	diameter, m
f	friction factor
G	mass velocity or mass flux, kg/m^2 s
g	gravitational acceleration, m/s^2
h	heat transfer coefficient, W/m^2 K
k	thermal conductivity, W/m K
L	length, m
p_{cr}	critical pressure, N/m^2
q	heat flux, W/m^2
T	temperature, °C or K

Greek symbols

ε	surface roughness, m
μ	dynamic viscosity, kg/m s
ρ	density, kg/m^3

Dimensionless number

Re	Reynolds number
Pr	Prandtl number
Nu	Nusselt number
Gr	Grashof number

Subscript

b	bulk temperature
f	film temperature
pc	pseudocritical
s	supercritical
w	wall temperature

supercritical pressure. During isobaric heat rejection process, CO_2 remains in gaseous like state, hence the heat exchanger is named gas cooler and single gaseous phase remains throughout the cycle. No condensation is associated with the cycle and smoother cooling profile is achieved during the cooling process. The heat transfer and pressure drop phenomenon in a gas cooler operating with CO_2 are completely different from traditional constant property fluids [13,14]. The coefficient of performance of a trans-critical refrigeration system is significantly influenced by the heat transfer from sCO_2 especially near the critical region [14]. For efficient designing of gas coolers, significant attention paid by the researchers for comprehensive and fundamental understandings of thermal and hydraulic behaviour of CO_2 operating under supercritical pressure. The supercritical carbon dioxide (sCO_2) differs completely from the traditional constant property refrigerants in terms of heat transfer mechanism and pressure drop near the critical pressure. Because of the aforementioned unique properties, sCO_2 is highly recommended for vapour compression refrigeration and air conditioning cycle, turbine reactor and heat pump.

Pitla et al. [15] reviewed the heat transfer and fluid flow characteristics of sCO_2 cooled in a horizontal tube. The correlations were compared applicable for cooling of sCO_2 in a gas cooler. Pioro et al. [16] reported a review of heat transfer correlations of sCO_2 for tubes and bundles and majority of the correlations failed to predict the deteriorated heat transfer upon heating of sCO_2. Duffey and Pioro [17] performed an exhaustive review of sCO_2 correlations in horizontal, vertical and other tube geometries. Correlations by various authors with the range of investigated parameters were listed. Three modes of heat transfer (normal heat transfer, deteriorated heat transfer and improved heat transfer) were proposed by comparing the correlations with experimental values. Cheng et al. [18] conducted excellent review work on sCO_2 correlations in micro and macro tube geometries. Heat transfer and pressure drop characteristics of sCO_2 cooled in a horizontal tube were discussed. The effect of lubricating oil on the heat transfer mechanism was also mentioned. Fang and Xu [19] compared the heat transfer accuracy of various correlations applicable for cooling of sCO_2 in horizontal tube and developed a new heat transfer correlation. Surendran et al. [20] performed comparison of various correlations of sCO_2 to predict the wall temperature, the bulk temperature and the heat transfer coefficient. Many of the existing correlations were not relevant to the experimental dataset. Further experimental investigations were suggested for better prediction of the wall and bulk temperatures. Lin et al. [21] reviewed the various heat transfer correlations of sCO_2 and performed the comparison of correlations with the experimental dataset. At significantly lower heat flux, most of the correlations showed better prediction while at higher heat flux, the buoyancy force became stronger and many of the existing correlations failed to predict the exact heat transfer mechanism. Gupta et al. [22] also performed comparison of existing correlations against various experimental dataset. Cheng et al. [23] investigated the comparison of various heat transfer correlations and the influence of different operating conditions on the heat transfer and pressure drop characteristics were also discussed. In Tables 1 and 2, experimental studies conducted by many researchers with sCO_2 in horizontal and vertical tubes are shown with the range of investigated parameters such as the inlet sCO_2 temperature, the operating pressure, the mass flux and the heat flux.

2. Research status and scopes

So far, the review works on the heat transfer correlations of sCO_2 have been conducted focusing specially on the comparison of the existing correlations with the experimental dataset. The influence of various operating parameters on the heat transfer mechanism and pressure drop characteristics for cooling of sCO_2 in various flow configurations was also reviewed. To the best of our knowledge, no review work has been conducted on the heat transfer mechanism and fluid flow behaviour for sCO_2 under both heating and cooling modes. A comprehensive understanding is required to predict the heat transfer mechanism and fluid flow behaviour for sCO_2 in a heat exchanger under both heating and cooling applications. The current paper presents a rigorous review of turbulent forced convection correlations for heat transfer and friction factor for supercritical CO_2 employed in horizontal tubes. The current review paper provides a good insight for evaluation of heat transfer performance and efficient design of a gas cooler or compact heat exchanger that has vast implementations in many engineering, chemical and power plant industries.

The scopes of the present article are described below.

(a) Heat transfer correlations in terms of average Nusselt number and friction factor correlations with their limits of applicability are comprehensively reviewed for sCO_2 applicable for in tube cooling/heating with horizontal orientation.
(b) The physical reasoning on the variation of different existing heat transfer correlations with experimental dataset is reported.
(c) The effect of mass velocity, the wall heat flux, the tube diameter, the operating pressure and temperature on the heat transfer mechanism and pressure drop characteristics are discussed.
(d) The possible physical reasoning behind the heat transfer deterioration under heating of sCO_2 is comprehensively discussed in the present article.
(e) The complex behaviour of the wall temperature distribution under

Table 1
Experimental studies of heat transfer and pressure drop of sCO_2 in horizontal tube.

Literature	Flow configuration	Inlet temperature (°C)	Inlet pressure (MPa)	Mass flux, G (kg/m^2 s)	Heat flux (kW/m^2)	Correlation proposed	Study content
Krasnoshchekov et al. [26]	(D = 2.64 mm, L = 150 mm)	29–214	8.0–12.0	NA	120–1110	Yes	HT
Krasnoshchekov et al. [27]	(D = 2.05 mm and 95 mm)	26–45	10	22,000	7500– 11,000	Yes	HT
Ankudinov and Kurganov [28]	(D = 8 mm, L = 1840 mm)	20	7.7	900–1540	2100–3200	No	HT
Pitla et al. [29]	(D = 4.72 mm)	91–126	7.79–13.42	NA	196–3870	Yes	HT & PD
Son and park [30]	(D = 7.75 mm)	90–100	7.5–10	200–400	NA	Yes	HT & PD
Yoon et al. [31]	(D = 7.73 mm)	50–80	7.5–8.8	225–450	NA	Yes	HT & PD
Liao and Zhao [24]	(D = 0.25–2.16 mm)	20–110	7.4–12	236–1179	NA	Yes	HT
Pitla et al. [32]	(D = 4.72 mm)	80–110	8–12	879–1795	NA	Yes	HT
Dang and Hihara [33]	(D = 1–6 mm)	30–70	8–10	200–1200	6–33	Yes	HT & PD
Oh and Son [25]	(D = 4.55 mm and 7.75 mm)	90–120	7.5–10	200–600	NA	Yes	HT
Fang [34]	(D = 0.79 mm, L = 530 mm)	25–65	8–12	200–1200	14–70	No	HT & PD
Huai et al. [35,36]	(D = 1.31 mm, L = 500 mm)	22–53	7.4–8.5	113.7–418.6	0.8–9	Yes	HT & PD
Pettersen et al. [37]	(D= 0.79 mm)	15–70	8.1–10.1	600–1200	NA	No	HT
Kuang et al. [38]	(D = 0.8 mm)	25–55	8–10	300–1200	NA	Yes	HT & PD
Olson [39]	(D = 10.9 mm)	20–126	7.8–13.4	200–900	NA	Yes	HT
Koppel and Smith [40]	(D = 4.93 mm, L = 457 mm)	18.3–48.9	7.38–7.58	NA	62.9–629.1	No	HT
Walisch et al. [41]	(D = 10 mm, L = 1500 mm)	50–120	8–10	80–500	0.4–2	No	HT & PD
Kuang et al. [42]	(D = 0.7 mm)	30–50	9	890	NA	No	HT & PD
Dang et al. [43]	(D = 1,2,4,6 mm)	20–70	8–10	200–1200	12–24	No	HT & PD
Yun et al. [44]	(D = 1 mm)	40–80	8.4–10.4	200–400	20–25	No	HT & PD
Mori et al. [45]	(D = 4 mm, 6 mm, 8 mm)	20–70	9.5	100–600	NA	Yes	HT
Kim et al. [46]	(D = 7.7 mm)	NA	7.5–8.5	215–430	11–18	Yes	HT
Kondou et al. [47]	(D = 6.1 mm)	91–126	7.5–8	100–240	NA	No	HT & PD
Zhao et al. [48]	(D = 1.98 mm and 4.14 mm)	20–100	8–11	400–1200	NA	Yes	HT
Gao and Honda [49]	(D = 5 mm)	20–100	7.6–9.6	330–680	NA	No	HT & PD
Zingerli and Groll [50]	(D = 2.75 mm)	100–125	8–12	1700–5100	NA	No	HT
Adebiyi and Hall [51]	(D = 22.1 mm, L =2.4 m)	10–31	7.6	35–150	5–40	No	HT
Melikpashaev [52]	(D = 4.5 mm, L= 457 mm)	7–102	9–12	NA	8000	No	HT

HT-heat transfer, PD-pressure drop, NA-not available.

heating of sCO_2 and the corresponding heat transfer deterioration are reported.

3. Thermo-physical properties of sCO_2

All the thermodynamic and transport properties of sCO_2 (density, specific heat, viscosity, thermal conductivity and Prandtl number) show extreme variation at pseudocritical temperature, which is one of the distinguish characteristics of sCO_2 in comparison with the constant property fluids. At pseudocritical temperature, the isobaric specific heat of fluid attains a peak value at a given pressure and it mimics the critical temperature. Near the pseudocritical temperature, sCO_2 shows rapid and nonlinear variation in the physical properties. Such drastic change in properties makes sCO_2 considerably different from constant property fluids. Fig. 1, shows the rapid and nonlinear property variation of sCO_2 at different operating pressures and temperatures. When the operating pressure increases, the pseudocritical temperature also increases and the variation of the properties are less dominant in the region distant from the critical condition. As the operating pressure approaches to the critical pressure, each property shows rapid and substantial change near the pseudocritical temperature. When sCO_2 is cooled in a gas cooler, the initial property variation is less and as the temperature reaches to pseudocritical point, there is a dramatic change in the properties. The peak of the specific heat becomes narrower and sharper as the operating pressure approaches to the critical pressure. The heat transfer coefficient shows significant augmentation during the gas cooling process. The sCO_2 is advantageous as a heat transfer fluid in the gas cooler compared to supercritical water due to its low critical parameters and lower value of specific volume. In a typical sCO_2 transcritical cycle, during cooling near to the critical temperature, along with specific heat, density also increases rapidly which causes the compressor to transfer a fluid with high density. Consequently, the compressing of high-density fluid by the compressor decreases the power consumption and increases the overall thermal performance of the cycle. Pseudocritical temperature is a function of operating pressure which can be calculated by the an algebraic equation where unit of operating pressure is bar and outcome is in terms of degree centigrade [24].

$$T_{pc} = -122.6 + 6.124p - 0.1657p^2 + 0.01773p^{2.5} - 0.0005608p^3 \quad (1)$$

4. Experimental studies

4.1. Experimental studies with sCO_2 cooling

A number of research studies on cooling with sCO_2 have been reported for horizontal tubes. Experiments have been performed to obtain the turbulent forced convective heat transfer and fluid flow characteristics near critical the condition (Liu et al. [1], Liao and Zhao [24], Oh and Son [25], Son and Park [30], Yoon et al. [31], Pitla et al. [32], Dang

Table 2
Experimental studies of heat transfer and pressure drop of sCO_2 in vertical tube.

Literature	Flow configuration	Inlet temperature (°C)	Inlet pressure (MPa)	Reynolds number, Re/Mass flux, G (kg/m² s)	Heat flux (kW/m²)	Correlation proposed	Study content
Jiang et al. [53]	(D = 2 mm)	55–70	7.8–9.8	Re = 4340, 6910, 8640	NA	No	HT & PD
Shiralkar and Griffith [54]	(D = 3.18 mm, 6.22 mm, L = 1520 mm)	10–32	7.6–7.9	Re = 267–835	125–190	No	HT
Shiralkar and Griffith [55]	(D = 3.18 & 6.35 mm, L = 1520 mm)	− 18–31	7.6–7.9	Re = 267–835	50–453	No	HT
Baskov et al. [56]	(D = 4.12 mm and L = 375 mm)	17–212	8–12	G = 1540–4170	< 640	Yes	HT & PD
Krasnoshchekov et al. [57]	(D = 4.08 mm, L = 208 mm)	22–45	10.32–10.75	NA	NA	Yes	HT
Bourke and Pulling [58]	(D = 22.8 mm, L = 4560 mm)	15–35	7.44–10.32	G = 311–1702	8–50	No	HT
Hiroaki et al. [59]	(D = 6 mm, L = 1000 mm)	0–170	8.1	G = 120–240	488;640	No	HT
Krasnoshchekov et al. [60]	(D = 4.08 mm, L = 208 mm)	20–110	7.9–9.8	G = 1135–7520	430–2520	Yes	HT
Krasnoshchekov et al. [61]	(D = 4.08 mm, L = 208 mm)	20–110	7.85–9.82	G = 350	< 2600	Yes	HT
Ikriannikov et al. [62]	(D = 29 mm, L = 2300 mm)	15–50	7.8–9.8	Re = 30×10^3–500×10^3	5.8–9.3	No	HT
Silin [63]	(D = 2.05 mm, L = 4.28 mm)	22–70	7.9–9.8	G = 200–2600	< 1100	No	HT
Jackson et al. [64]	(D = 19.05 mm, L = 2460 mm)	8–20	7.25–8.27	G = 5–57	100–560	No	HT & PD
Fewster and Jackson [65]	(D = 5.08 mm, 7.88 mm, L = 1200 mm)	10	7.6	G = 50–460	300–3300	No	HT & PD
Surendran et al. [20]	(D = 0.948–9 mm)	5–32	7.58–9.59	G = 400–1641	20–225	No	HT
Bruch et al. [66]	(D = 6 mm, L = 750 mm)	15–70	7.4–10.2	Re = 3600–1.8×10^6	NA	Yes	HT
Liao and Zhao [67]	(D = 0.74 mm, 1.4 mm, 2.16 mm, L = 110 mm)	20–110	7.4–12	G = 1.2–12, Re = 10^4-2×10^5	NA	Yes	HT
Bae and Kim [68]	(D = 4.4 & 9 mm, L = 3000 mm)	5–27	7.75–8.85	G = 400–1200	100–150	Yes	HT
Gupta et al. [69]	(D = 8 mm, L = 2208 mm)	20–40	7.4–8.8	G = 900–3000	15–615	Yes	HT
Jiang et al. [70]	(D = 2 mm L = 39 mm)	23–35	7–12	Re < 2500	4.49–94	No	HT
Jiang et al. [71]	(D = 4 mm , L = 50 mm)	30–45	7.7–12	Re < 3500	2.29–89	Yes	HT & PD
Bae at al. [72]	(D = 6.32 mm, L = 2650 mm)	80–100	7.75–8.12	Re = 1.8×10^4–3.8×10^5	30–170	Yes	HT & PD
Kim et al. [73]	(D = 4.4 & 9 mm L = 1800 mm)	30–120	7.75	G = 400–1200	30–50	Yes	HT
Kim et al. [74]	(D = 7.8 mm L =1800 mm)	15–32	8	G = 209–1230	3–180	Yes	HT
Kurganov and Kaptilnyi [75]	(D = 22.7 mm L = 5220 mm)	25–35	9	G = 800–1200	40–260	No	HT
Fewster [76]	(D = 8 mm, L = 1000 mm)	10–25	7.6	G = 180–2000	10–300	No	HT

HT-heat transfer, PD-pressure drop, NA-not available.

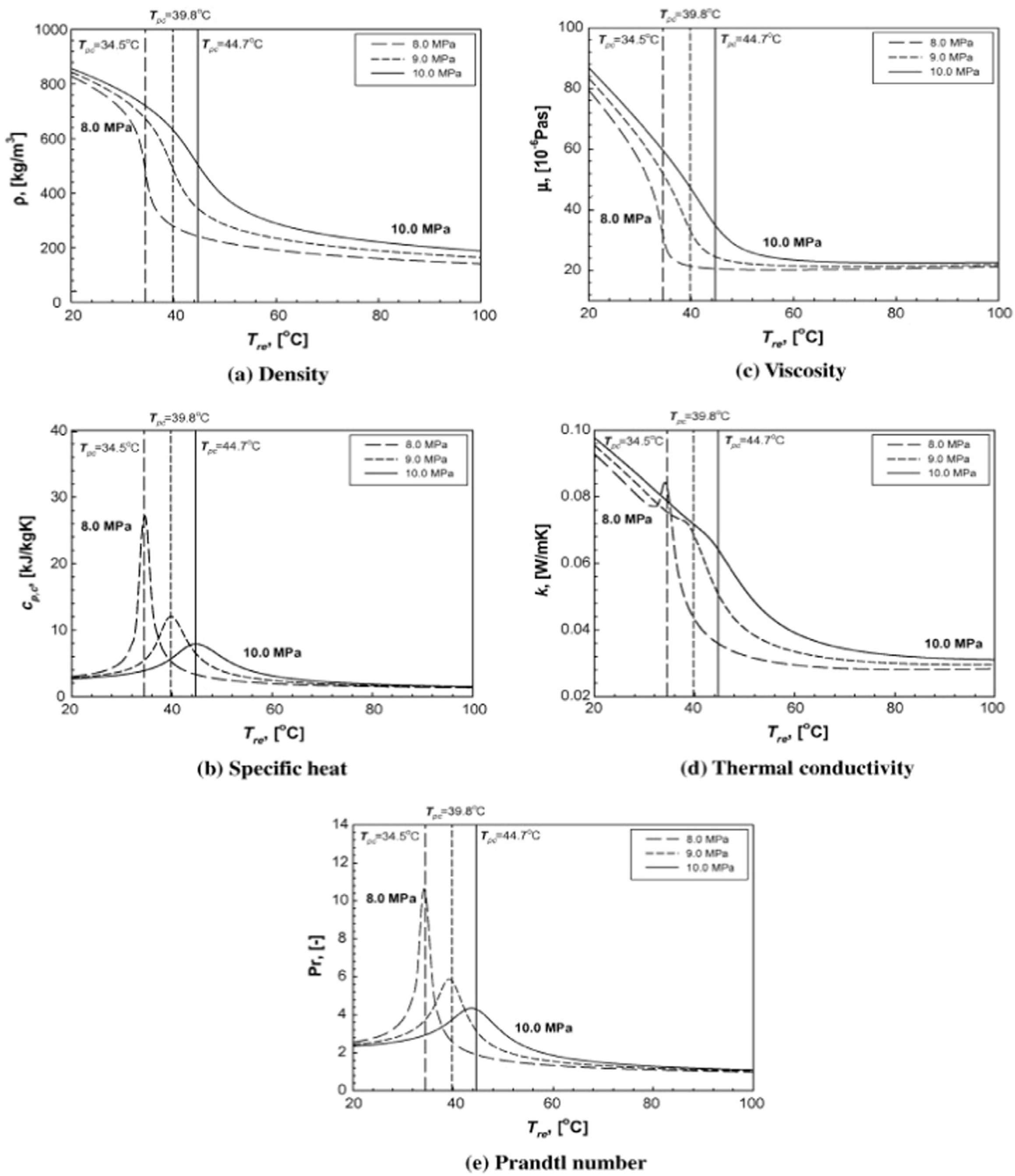

Fig. 1. Physical property variation of sCO_2 at different temperature and pressure [25].

and Hihara [33], Huai et al. [35], Bruch et al. [66]). The review of experimental studies on sCO_2 cooling is essential in the present articles due to the following reasons.

(a) For thermally efficient design of heat exchanger, the understandings of heat transfer and pressure drop characteristics of sCO_2 are essential operating under cooling condition with horizontal orientation of circular tubes.
(b) The heat transfer performance near the critical region depends on the mass flux, the heat flux, the inlet fluid temperature and the operating pressure. These experimental studies demonstrated the significant influence of operating parameters especially on the heat transfer and friction factor characteristics.
(c) Since sCO_2 proves to be a promising candidate as a working fluid in thermal and nuclear power plants, the review of these experimental studies is essential in designing more efficient and compact heat exchangers working under supercritical conditions during cooling process.

Liu et al. [1] employed circular tubes of 4, 6 and 10.7 mm of inner diameter to experimentally examine the heat transfer and pressure drop of sCO_2 cooled for a range of inlet fluid temperature 25–67 °C, the inlet pressure 7.5–8.5 MPa and the mass flow rate 0.35–0.8 kg/min. An increase of mass velocity augmented the heat transfer coefficient. Based on their experimental findings, a correlation was developed for circular tube in terms of average Nusselt number. Liao and Zhao [24] reported experimental study of sCO_2 cooling in a horizontal stainless steel circular tube of diameter 0.5–2.16 mm. This study was performed for a range of pressure 7.4–12 MPa, the inlet temperature 20–110 °C and the mass flow rate 0.02–0.2 kg/min. Buoyancy force was significant up to

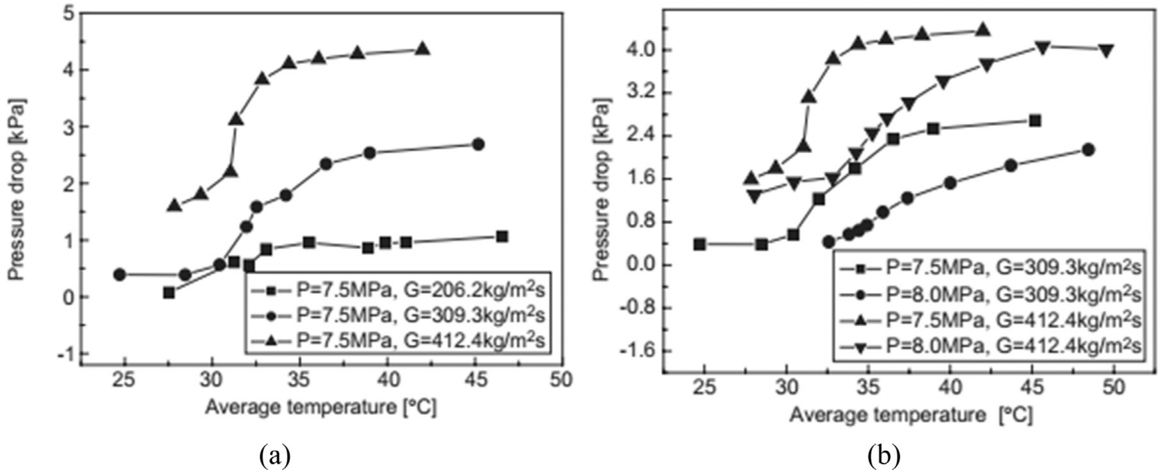

Fig. 2. Variation of pressure drop at different mass flux by Huai et al. [35].

Reynolds number 10^5 and was less dominant with reduced tube diameter. A correlation was proposed for circular tube with a mean relative error of 9.8%. Oh and Son [25] experimentally obtained the convective heat transfer coefficient during sCO_2 cooling process in a horizontal tubes of inner diameter of 4.55 and 7.75 mm. The study indicated that during cooling of sCO_2 near critical region, the heat transfer coefficient significantly affected by the operating temperature, pressure, the tube diameter and the mass velocity. A heat transfer correlation was proposed applicable for inlet pressure of 7.5–10 MPa, mass flux 200–600 kg/m^2 s and inlet fluid temperature 90–100 °C.

Son and Park [30] performed experiments to observe the heat transfer and fluid flow behaviour in a circular tube of diameter 7.75 mm and length of 500 mm and reported a heat transfer correlation. The convective heat transfer coefficient exhibited a highest value at the pseudocritical temperature and pressure drop during the cooling process decreased with the increased inlet pressure due to less variation of properties in region further away from the critical condition. Yoon et al. [31] conducted experiment to report the heat transfer and the characteristics of pressure drop in a horizontal copper tube of 7.73 mm of diameter operating under mass flux 225–450 kg/m^{2}s, the bulk temperature 50–80 °C and the operating pressure 7.5–8.8 MPa. As the bulk fluid temperature approached to pseudocritical temperature, the convective heat transfer coefficient showed significant improvement. The pressure drop reduced when the operating pressure was increased from the critical condition. A heat transfer correlation was proposed where the properties evaluated at bulk temperature. Pitla et al. [32] proposed a new heat transfer correlation in terms of Nusselt number for sCO_2 cooling in a horizontal tube based on their experimental and numerical findings. Experiments conducted with a circular tube of 6.35 mm diameter and length of 1300 mm for a range of inlet pressure 9.4–13.4 MPa, the inlet temperature 20–124 °C and the mass flow rate 0.02–0.039 kg/s. The proposed correlation for the Nusselt number was the mean value of Nusselt number evaluated at bulk and wall temperature. Dang and Hihara [33] experimentally observed the influence of various operating parameters on the heat transfer mechanism in a horizontal tube of diameter 1–6 mm. When the bulk fluid temperature was less than the pseudocritical temperature, the heat transfer coefficient was relatively unchanged with increased heat flux. Increased tube diameter improved the heat transfer performance and the operating heat flux beyond the optimum value showed negative influence on the heat transfer rate. A heat transfer correlation was developed by the modification of Gnielinski correlation.

Huai et al. [35] experimented with sCO_2 to examine the fluid flow and heat transfer mechanism in a horizontal tube of 1.31 mm inner diameter. Both local and average Nusselt number were calculated for a range of operating pressure 7.4–8.5 MPa, the inlet sCO_2 temperature 22–53 °C and the mass flux 113.7–418.6 kg/m^2 s. Near critical region, both heat transfer rate and friction factor augmented with increased mass flux but reduced with increased operating pressure. Based on their investigation, a new correlation was recommended suitable for forced convection under cooling condition. Bruch et al. [66] presented an experimental work with sCO_2 on heat transfer mechanism with an effect of buoyancy force in a vertical tube configuration with a copper tube of 6 mm diameter. Experiments conducted for a range of mass flux 50–590 kg/m^{2}s, the pressure 7.4–12 MPa, the inlet temperature 15–70 °C and the Reynolds number 3600–1.8 × 10^6 and correlation developed for upward and downward flow. For upward flow, increased mass flux improved the heat transfer rate where as for downward flow, a limit of mass flux was found below which the heat transfer augmented due to the role played by the free convection.

4.1.1. Pressure drop characteristics

Huai et al. [35] performed experimentation to investigate the sCO_2 flow behaviour in a circular pipe of inner diameter 1.31 mm. In Fig. 2(a), when the bulk mean temperature of sCO_2 gradually increased from the pseudocritical temperature (31.7 °C for 7.5 MPa and 34.63 °C for 8 MPa), pressure drop increased as well. Near the pseudocritical temperature, variation of pressure drop was drastic due to the severe change of thermos-physical properties. Increasing the mass flux from 206.2 to 412.4 kg/m^2 s, caused increased pressure drop at the same operating pressure. In Fig. 2(b), when the operating pressure was increased from the critical pressure (7.5–8 MPa) with the same mass flux, the pressure drop decreased due to less variation of properties away from the critical region. The influence of mass velocity on the pressure drop was also experimentally investigated with different diameters of a circular pipe by Son and park [30], Yoon et al. [31], Pettersen [37], Kuang et al. [42], Yun et al. [44], Zingerli and Groll [50], Liu et al. [1] and Fang et al. [77] and reached similar findings.

4.1.2. Heat transfer characteristics

The influence of the operating pressure and the mass flux on the characteristics of turbulent forced convective heat transfer coefficient with the change of bulk mean fluid temperature is shown in Fig. 3. For a mass flux of 206.2 kg/m^{2}s, the heat transfer coefficient reached a maximum value when the bulk temperature of sCO_2 reached the pseudocritical temperature and dropped sharply in the region further away from the critical condition, shown in Fig. 3(a). The substantial improvement of heat transfer was due to the fact that specific heat constant was maximum at pseudocritical temperature. As the operating pressure was increased from the critical region, heat transfer coefficient decreased due to less dominant property variation further away from the critical region. The mass flux significantly influenced the heat

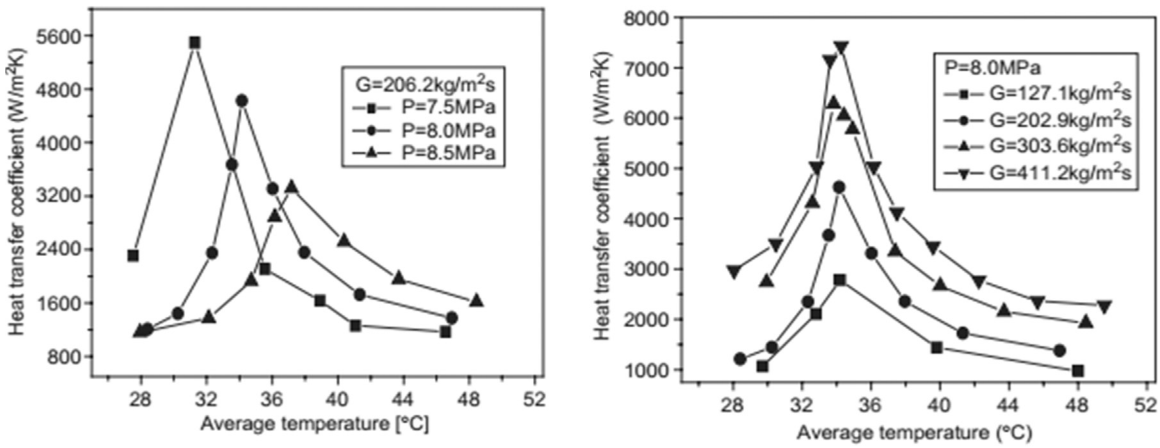

(a) (b)

Fig. 3. Influence of pressure and mass velocity on the local heat transfer coefficient (Huai et al. [35]).

transfer behaviour as shown in Fig. 3(b). The higher the values of mass velocity, the greater the augmentation of heat transfer at a fixed operating pressure due to the augmentation of turbulent diffusion. Similar conclusion of heat transfer characteristics were observed from experimental studies performed by Son and park [30], Yoon et al. [31], Pettersen [37], Olson [39], Kuang et al. [42], Liao and Zhao [24], Kim et al. [73] and many more.

4.1.3. Effect of tube diameter

The influence of tube diameter on the forced convection heat transfer performance at a same mass flux and operating pressure was reported by Oh and Son [25] during the gas cooling process. The experiment conducted with two circular tubes of inner diameter of 4.55 mm and 7.75 mm. In Fig. 4, the convective heat transfer coefficient $h_{gc,\,loc}$ variation with bulk mean temperature T_{re} by the influence of tube diameter is shown. Due to the increase of heat transfer contact area, the reduction of tube diameter caused considerable increment of heat transfer. At mass velocity, $G_{re} = 400\,\mathrm{kg/m^2\ s}$ and pressure $P_{in} = 10\,\mathrm{MPa}$, the heat transfer rate augmented by 8–35.6% when the tube diameter was decreased from 7.75 mm to 4.55 mm. The unique heat transfer mechanism of sCO_2 suggests the employment of gas cooler with smaller diameter working under higher operating pressures without excessive wall thickness. Dang and Hihara [33], Pettersen [37], Dang et al. [43] and Kim et al. [46] also confirmed the improvement of heat transfer rate with the reduced diameter pipe.

4.1.4. Effect of buoyancy

The buoyancy force considerably affects the heat transfer performance and pressure drop characteristics depending on the operating conditions and flow orientation. For vertically upward flow, heat transfer deterioration or impairment is observed depending on the flow condition whereas for downward and horizontal flow, buoyancy force aids the heat transfer rate due to the earlier transition from laminar to turbulent flow. The effect of buoyancy on the heat transfer behaviour was comprehensively investigated by Liao and Zhao [67], Jackson et al. [64], Bruch et al. [66], Bae and Kim [68], Jiang et al. [71], Bae et al. [72], Kim et al. [73], and Jackson and Hall [78]. According to Bruch et al. [66], the influence of buoyancy force in a vertically upward and downward flow during cooling process, became significant when the semi-empirical parameter (modified form of Richardson number, developed by Jackson and Hall [78]) $\frac{Gr}{Re^{2.7}}$ was more than 10^{-5}.

In Fig. 5, the dotted line represents the limiting value of the buoyancy parameter, above which mixed convection significantly affected the heat transfer performance. When the mass flux was high enough (G = 400 kg/m² s), buoyancy force was less dominant and forced convection became influential on the overall heat transfer mechanism. At moderate and lower values of mass flux (G = 200 kg/m² s), in the high density region of sCO_2, when the bulk temperature was below the pseudocritical temperature, buoyancy parameter became significant and mixed convection considerably affected the heat transfer mechanism. In the gas like region, where the bulk temperature was above the pseudocritical temperature, forced convection was the main mechanism. For the lowest mass flow rate, free convection was noticed for the whole range of bulk temperatures.

4.2. Experimental studies with sCO_2 heating

Heat transfer to supercritical CO_2 under heating condition in circular tubes have been extensively studied by many researchers over the last few decades due to extreme demand in many engineering and industrial application (Liao and Zhao [67], Bae and Kim [68], Gupta et al. [69], Jiang et al. [71], Bae et al. [72], Kim et al. [73], Kim et al. [74], Scalabrin and Piazza [79]). The review of experimental studies on sCO_2 heating is essential in the present articles due to the following reasons.

(a) The sCO_2 application in heating mode is completely different as the operating heat flux and the mass velocity significantly influence the overall heat transfer behaviour.
(b) Unlike from cooling of $sCO_{2,}$ the heat transfer improvement is dependent on certain local conditions. On top of that, three modes of heat transfer (normal, improved and deteriorated) are observed during heating of $sCO_{2.}$

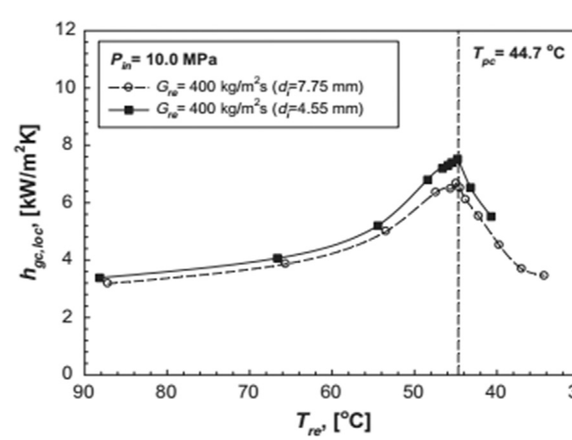

Fig. 4. Influence of tube diameter on heat transfer performance in cooling mode (Oh and Son [25]).

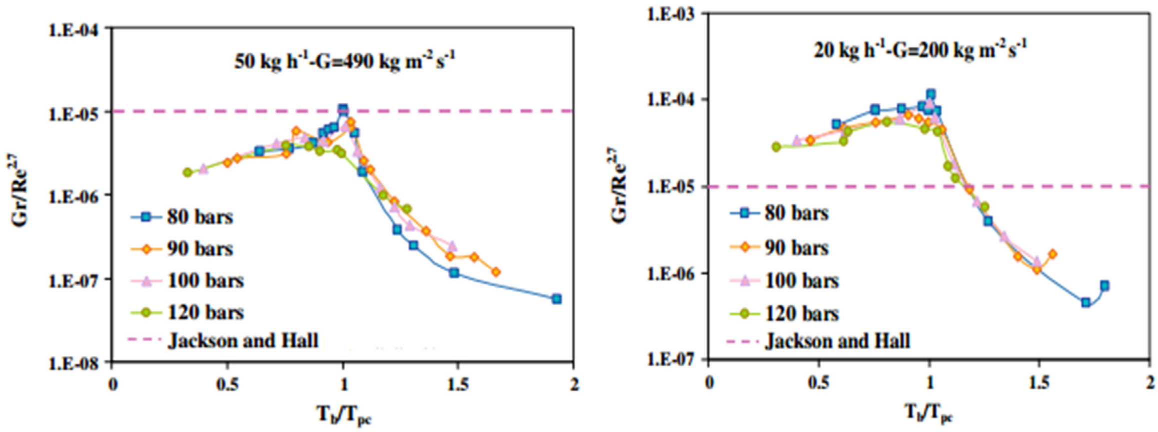

Fig. 5. Influence of buoyancy for vertically downward flow at low and high mass flux (Bruch et al. [66]).

(c) The irregular and unpredicted wall temperature distribution are only relevant to heating of sCO_2. The experimental studies can only explain this complex phenomenon.
(d) The proper condition on the development of heat transfer deterioration is still an unsolved mystery during heating of sCO_2 in various flow configuration. The experimental as well as fundamental understandings are required to address this complex phenomenon of heat transfer deterioration.

Liao and Zhao [67] performed experimentation to observe the convection heat transfer to sCO_2 heated in a vertical and horizontal miniature circular tubes of inner diameter of 0.70, 1.4 and 2.16 mm under turbulent flow condition. Experiments performed for a range of pressures 7.4–12 MPa, the inlet temperature 20–110 °C, the mass flow rate 0.02–0.2 kg/min, the Reynolds number 10^4 to 2×10^5 and the Prandtl number 0.9–10. Buoyancy force had a significant influence on the heat transfer mechanism. For downward flow, the heat transfer performance reduced known as deteriorated heat transfer, whereas for upward and horizontal flow, the heat transfer rate increased under the same flow condition. Based on their experimental findings, heat transfer correlations for upward, downward and horizontal flow were proposed by incorporating the effect of buoyancy in the correlation. Bae and Kim [68] investigated the heat transfer behaviour of heating of sCO_2 in a vertically upward flow of a circular tube of 4.4 and 9 mm diameter and in an concentric annular tube of 8 mm inner diameter. Experiment conducted for a range of pressure 7.75–8.85 MPa, the inlet fluid temperature 5–27 °C, the mass flux 400–1200 kg/m^2 s and the heat flux applied on the wall boundary was up to 150 kW/m^2. The heat transfer correlation was proposed by taking account of buoyancy parameter. It showed good agreement with the experimental dataset for normal heat transfer regime and degraded heat transfer regime for some cases.

Gupta et al. [69] developed heat transfer correlations applicable for heating of sCO_2 in a vertically bare tube of 8 mm internal diameter and 2208 mm in length by adapting the mean bulk, the mean wall and the mean film temperature approach. Experiments conducted with inlet pressure ranging from 7.4 to 8.8 MPa, the inlet temperature 20–40 °C, the mass flux 900–1300 kg/m^2 s and the heat flux 15–615 kW/m^2. The rapid variation of properties near the critical region was reasonably captured by the correlations. Correlation based on mean wall temperature showed better prediction with the experimental data in comparison with correlations based on the bulk and film temperature. Jiang et al. [71] performed experimentation to obtain the heat transfer and fluid flow behaviour in a circular tube with vertical orientation. The local heat transfer coefficient, the friction factor and the wall temperature profile for different flow conditions like the inlet pressure, temperature, the buoyancy force and the flow direction were reported. Bae et al. [72] reported an experimental study of sCO_2 heated in a vertical circular tube of 6.32 mm of diameter to observe the influence of the Reynolds number, the heat flux and the buoyancy force on the heat transfer mechanism. The study carried out for a range of pressure 7.75–8.12 MPa, the heat flux 30–170 kW/m^2, the mass flux 285–1200 kg/m^{2}s and the Reynolds number 1.8×10^4 to 3.8×10^5. The thermal acceleration and buoyancy force caused M shape velocity profile and sharp gradient of shear stress near the wall. As a consequence, heat transfer deterioration occurred for upward flow direction. Correlations were proposed for both average Nusselt number and friction factor for normal heat transfer and deteriorated heat transfer regimes applicable for upward and downward flow in a vertical tube.

Kim et al. [73] performed experimentation to explore the influence of the mass flux, the heat flux and other operating condition on the wall temperature profile and heat transfer effectiveness in a tube of 4.4 and 9 mm of inner diameter and through a narrow concentric annular space. Based on experimental findings, a heat transfer correlation was reported by incorporating the influence of buoyancy force for the normal heat transfer and the deteriorated heat transfer regimes. The wall temperature profile in stream wise direction and the heat transfer characteristics were experimentally investigated with supercritical CO_2 heated in channels with circular, triangular and square cross-sections under turbulent flow condition (Kim et al. [74]). The wall temperature profile took an earlier peak value which caused earlier heat transfer deterioration for non-circular cross sections compared to circular cross-section under the same heat flux. Scalabrin and Piazza [79] applied the neural network method to model the turbulent heat transfer to sCO_2 heated in a horizontal tube and studied the influence of the mass flux, the heat flux, the inlet temperature and pressure on the characteristics of the heat transfer and validated their findings with experimental dataset. The study performed for a range pressure 9.8–12.6 MPa, the temperature 28–32 °C, the mass flux 170–910 kg/m^2 s and the heat flux 12–66 kW/m^2.

4.2.1. Effect of tube diameter

Opposite trend of the effect of tube diameter on the forced convection heat transfer behaviour under heating of sCO_2 were observed by Liao and Zhao [67], Bae and Kim [68], and Kim et al. [73]. During heating of sCO_2, the average Nusselt number was improved with an increase of tube diameter due to the possible effect of buoyancy force, reported by Liao and Zhao [67] with an experimental study of heating of sCO_2 in a circular pipe of inner diameter 0.70, 14 and 2.16 mm. In Fig. 6, the heat transfer performance in terms of average Nusselt number increased with increased tube diameter. Similar behaviour of heat transfer rate was observed with vertically upward and downward flow in a tube. It is hard to draw conclusion on the influence of tube diameter on the local heat transfer coefficient during heating and cooling modes as very few experimental studies have been found from the literature. The above comparison was made with same mass flux but

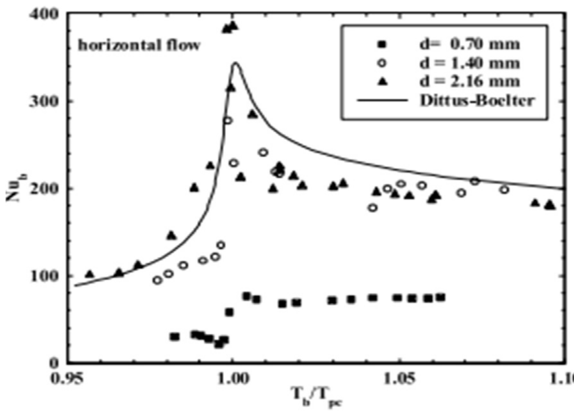

Fig. 6. Influence of tube diameter on heat transfer performance in heating mode (Liao and Zhao [67]).

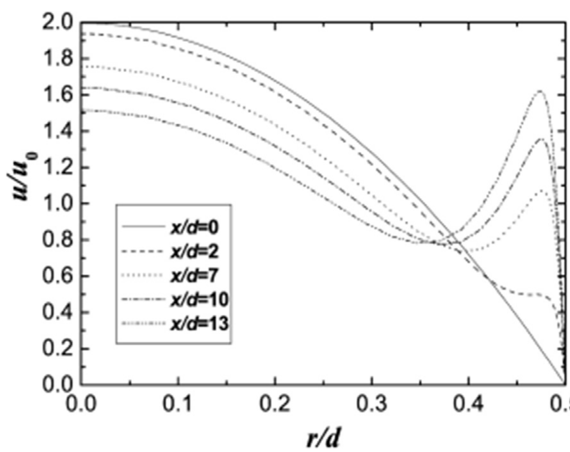

Fig. 7. Velocity distribution at various location of tube (Jiang et al. [70]).

an increase or decrease of tube diameter certainly changes the flow Reynolds number. Therefore, it is recommended that instead of mass flux, same Reynolds number could be a good criterion to examine the influence of tube size on the heat transfer performance.

4.2.2. Heat transfer deterioration in heating mode

The heat transfer deterioration might occur during heating of supercritical CO_2 under certain flow conditions such as the high heat flux or the high wall temperature, the sharp decrease of density just above the pseudocritical temperature and the low mass velocity which is reflected by distorted velocity pattern in peripheral direction of pipe caused by the distortion of shear stress at the wall boundary [28]. As the heat was applied at the wall, when the bulk fluid temperature near the wall reached the pseudocritical temperature, M shape velocity distribution along the radial direction and steep shear stress distribution were observed. This reduction of turbulent production was due to the local laminarization [75]. According to Shiralkar and Griffith [54], the heat transfer deterioration observed when the wall temperature was higher and the bulk fluid temperature was lower than the pseudocritical temperature. When the buoyancy force became stronger, the velocity at viscous sublayer became faster compared to the velocity in the core region and developed negative shear stress at the wall boundary. Therefore, the wall temperature exhibited a peak value due to the degraded heat transfer significantly influenced by the buoyancy force under certain heat flux and mass velocity. Depending on the operating pressure and the mass velocity, a limit of heat flux existed over which heat transfer rate significantly degraded [55]. Jiang et al. [70] reported experimental and numerical studies to observe the influence of the wall heat flux on heat transfer deterioration with sCO_2 in a circular vertical

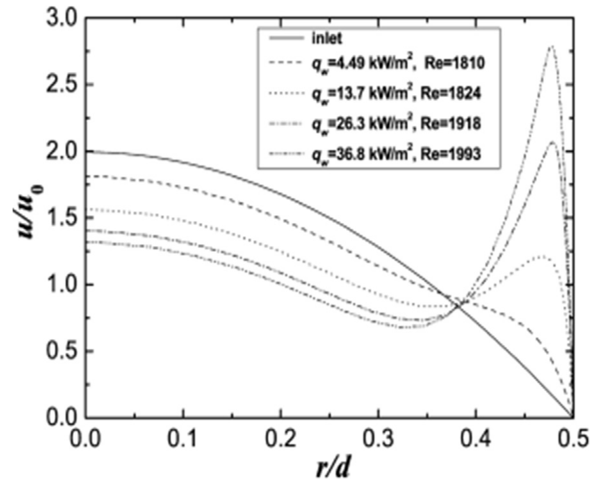

Fig. 8. Velocity distribution with varying heat flux at tube location x/d = 10 (Jiang et al. [70]).

tube at various location. In Fig. 7, deformation of velocity profile at various tube location is shown for the tube wall temperature 35 °C, $Re = 2360$, $P = 9.52$ MPa, $G = 6.34\ kg/m^2\ s$, $q = 13.0\ kW/m^2$. The formation of M shape velocity profile was due to the abrupt decrease of density, flow accelerated near wall region, as a result velocity gradient between the tube core and the viscous sublayer reduced. As a consequence, this reduced turbulent production ultimately caused the heat transfer deterioration. In Fig. 8, as the heat flux was increased from 4.49 to 36.8 kW/m^2, the distortion of the velocity distribution was more severe at a tube location $x/d = 10$, wall temperature 24.6 °C, $G = 6.39\ kg/m^2$ s and $P = 9.57$ MPa. The phenomenon of reduction of heat transfer rate with increased heat flux was due to the reduction of transport properties of sCO_2 at a temperature higher than pseudocritical temperature and local laminarization due to the strong influence of buoyancy. Ankudinov and Kurganov [28], Bourke and Pulling [58] , Bae et al. [72] and Kurganov and Kaptilnyi [75] also performed experimentation to study the heat transfer deterioration by the influence of buoyancy and other flow parameters.

4.2.3. Effect of wall temperature distribution

The influence of the wall temperature on the heat transfer mechanism is substantially important particularly under heating of sCO_2 in a circular tube. When the ratio of the wall heat flux to the mass velocity increases beyond a critical value, the wall temperature exhibits an earlier peak and causes the heat transfer deterioration due to the reduction of turbulent production in the near wall regime. When the wall temperature is beyond the pseudocritical temperature, there is a sharp decrease of density of sCO_2. As a result, the reduction of velocity gradient between tube core and boundary causes distortion of shear stress and significant reduction of turbulent production. Kim et al. [73] observed such scenarios of increased wall temperature profile and degraded heat transfer in a tube of 4.4 mm diameter, where sCO_2 heated under various heat and mass flux. In Fig. 9, the wall temperature distribution with the bulk fluid enthalpy is shown for three cases (Case A1: $G = 400\ kg/m^2$ s, $q = 30\ kW/m^2$, Case A2: $G = 400\ kg/m^2$ s, $q = 50\ kW/m^2$, Case A3: $G = 1200\ kg/m^2$ s, $q = 50\ kW/m^2$). For case A1 and A3, the wall temperature augmented monotonously with the bulk fluid temperature and improved heat transfer was obtained. For case A2, earlier peak of the wall temperature took place, when the wall temperature approached pseudocritical temperature and bulk fluid temperature was still lesser than the pseudocritical temperature. The deterioration of heat transfer observed until the bulk temperature reached the pseudocritical temperature.

The wall temperature profile with the increased heat flux investigated for circular, triangular and square channel is shown in

Fig. 10 along the channel length by Kim et al. [74] for a mass velocity of 628 kg/m^2 s. As the heat flux was increased, the wall temperature suddenly rose at the pseudocritical temperature and caused heat transfer degradation. In case of triangular and square channel, the wall temperature took earlier peak at significantly higher heat flux in comparison with circular channel.

5. Numerical studies with sCO_2

Pitla et al. [29,32] performed numerical investigation with sCO_2 cooled in a circular tube of 4.72 mm of diameter and simulation results showed good agreement with the experimentally obtained convective heat transfer coefficient and pressure drop values. Two methods were employed to solve the complex turbulence model: density weighted averaging and time averaging. Comparing their numerically predicted values with experimental findings, a heat transfer correlation in terms of Nusselt number was proposed. Jiang et al. [53] performed comparison of their experimental findings with numerical simulation with sCO_2 cooled in a vertical tube of 2 mm diameter. The influence of the sCO_2 mass flow rate, the water mass flow rate and the other operating parameters on the heat transfer performance and friction factor were investigated. The Buoyancy effects were well captured by the numerical simulation for both upward and downward flow. Jiang et al. [70] reported experimental and numerical findings with sCO_2 heated in a vertical tube of 2 mm diameter for small range of Reynolds number (less than 2500). The influence of the mass velocity, the heat flux, the operating temperature, the gravity and the flow direction were thoroughly investigated on the pressure drop and the heat transfer mechanism. Two dimensional steady state laminar governing equations for mass, momentum and energy were considered for the simulation model. For vertically upward flow, the wall temperature changed in a complex nonlinear manner whereas for vertically downward flow, wall temperature augmented monotonically with the applied heat flux. Wang and Hihara [80] performed numerical simulation of sCO_2 cooling in a counter flow concentric heat exchanger to explore the influence of the mass velocity, the heat flux, the operating temperature and pressure on the local and average heat transfer coefficient. Radial distribution of thermodynamic and transport properties of sCO_2 was reported along the fluid flow path and heat transfer data was compared with the existing correlations. Kruizenga et al. [81] conducted experimentation and numerical modelling to investigate the heat transfer and the fluid flow behaviour of sCO_2 cooled in a semi-circular channel of 1.9 mm of diameter and 500 mm of length by employing commercially available CFD software, ANSYS Fluent. The turbulent forced convection heat transfer rate considerably improved with an increase of the flow Reynolds number, the Prandtl number and decreased with the operating pressure. The simulation findings showed reasonable agreement with the experimental findings. The study performed for a range of pressure 7.5–10.1 MPa, the Reynolds number up to 100 K. Different turbulent models were employed to predict the wall temperature profile, among which the turbulent viscosity SST k-ω model was chosen for comparison with experimental findings. Based on experimental and numerical findings, a correlation for average Nusselt number was proposed by modifying the Jackson and Hall [78] correlation and incorporating ratio of bulk specific heat to specific heat of an ideal gas. Petrov and Popov [82] developed both heat transfer and friction factor correlations applicable for gas cooling of sCO_2 in a horizontal channel based on their experimental and numerical studies. Lee and Howell [83] performed numerical computation of sCO_2 and supercritical water cooled in a circular tube with vertical orientation. The variation of thermodynamic and transport properties with the bulk fluid temperature and mass flow rate were investigated. The fluctuating density k-ε turbulent model was employed and the variation of density with the bulk fluid enthalpy was incorporated in to the governing continuity, momentum and energy equations. The simulation results showed good agreement with experiments. Zhang and Yamaguchi [84] performed numerical study of forced convection heat transfer of sCO_2 for the Reynolds number ranges from 210 to 1800. The study performed with a circular tube of 6 mm diameter, the operating sCO_2 pressure 8 MPa, the inlet temperature

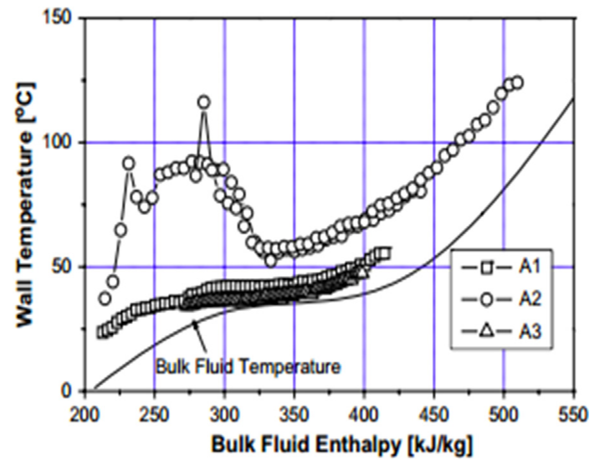

Fig. 9. The wall temperature profile under varying heat and mass flux (Kim et al. [73]).

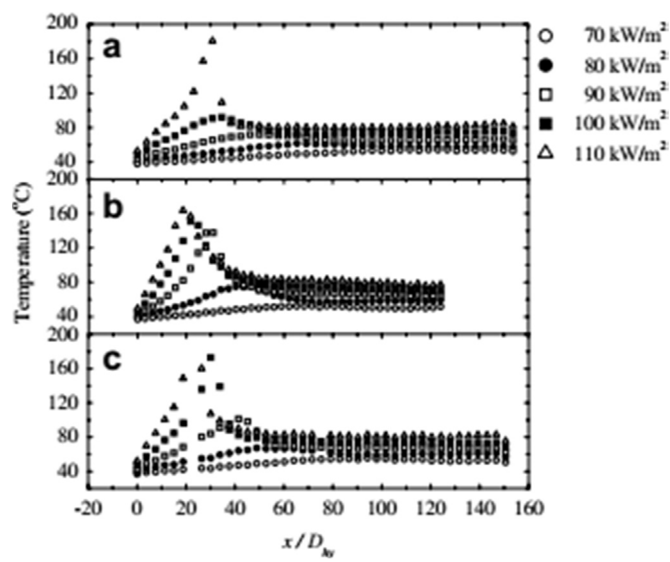

Fig. 10. Wall temperature profile for circular (a), triangular (b) and square (c) channel (Kim et al. [74]).

Table 3
Values for coefficients in Krasnoshchekov et al. [26] correlation.

P (MPa)	8	10	12
n	0.38	0.68	0.8
B	0.75	0.97	1.0
L	0.18	0.04	0

Table 4
Values of m and n in Baskov et al. [56] correlation.

	$\frac{\overline{C_p}}{C_{pw}}>1$			$\frac{\overline{C_p}}{C_{pw}}\leq 1$		
P (MPa)	8	10	12	8	10	12
m	1.2	1.6	1.6	0.45	0.45	0.45
n	0.15	0.1	0	0.15	0.1	0

Table 5
Review of sCO_2 heat transfer correlations.

Literature	Tube geometry	Correlation
Liu et al. [1]	(D = 4, 6 and 10.7 mm)	$Nu = 0.01Re_w^{0.9}Pr_w^{0.5}\left(\frac{\rho_w}{\rho_b}\right)^{0.906}\left(\frac{Cp_w}{Cp_b}\right)^{-0.585}$
Oh and Son [25]	(D = 4.55 mm and 7.75 mm)	$Nu = 0.023Re_b^{0.7}Pr_b^{2.5}(\frac{Cp_b}{Cp_w})^{-3.5}$ for $T_b < T_{pc}$ $Nu = 0.023Re_b^{0.6}Pr_b^{3.2}\left(\frac{\rho_b}{\rho_w}\right)^{3.7}\left(\frac{Cp_b}{Cp_w}\right)^{-4.6}$ for $T_b \geq T_{pc}$
Son and park [30]	(D = 7.75 mm, L = 500 mm)	$Nu = Re_b^{0.55}Pr_b^{0.23}(\frac{Cp_b}{Cp_w})^{0.15}$ For $T_b/T_{pc} > 1$ $Nu = Re_b^{0.35}Pr_b^{1.9}\left(\frac{\rho_b}{\rho_w}\right)^{-1.6}\left(\frac{Cp_b}{Cp_w}\right)^{-3.4}$ For $T_b/T_{pc} \leq 1$
Yoon et al. [31]	(D = 7.73 mm)	$Nu = 1.38Nu_w\left(\frac{\rho_w}{\rho_b}\right)^{0.57}\left(\frac{\overline{Cp}}{Cp_w}\right)^{0.86}$ Where, Nu_w calculated by Gnielinski [88] equation. $Nu_w = \frac{(\frac{f_w}{8})(Re_w-1000)Pr_w}{1.07+12.7\left(\frac{f_w}{8}\right)^{0.5}(Pr_w^{\frac{2}{3}}-1)}$ The authors [31] then simplified the correlation. $Nu = aRe_b^{\,b}Pr_b^{\,c}\left(\frac{\rho_{pc}}{\rho_b}\right)^n$ a = 0.14, b = 0.69, c = 0.66, n = 0 for $T_b > T_{pc}$ a = 0.013, b = 1.0, c = -0.05, n = 1.6 for $T_b \leq T_{pc}$
Pitla et al. [29,32]	(D = 4.72 mm)	$Nu = \frac{Nu_w + Nu_b}{2}(\frac{k_w}{k_b})$ Where Nu_w and Nu_b are average Nusselt number evaluated by Gnielinski [88] correlation evaluated at T_w and T_b respectfully.
Dang and Hihara [33]	(D = 1–6 mm)	$Nu = \frac{(\frac{f_f}{8})(Re_b-1000)Pr}{1.07+12.7\left(\frac{f_f}{8}\right)^{0.5}(Pr^{2/3}-1)}$ $Pr = \begin{cases} \frac{Cp_b\mu_b}{k_b}; Cp_b \geq \overline{Cp} \\ \frac{\overline{Cp}\mu_b}{k_b}; Cp_b < \overline{Cp} and \frac{\mu_b}{k_b} \geq \frac{\mu_f}{k_f} \\ \frac{\overline{Cp}\mu_f}{k_f}; Cp_b < \overline{Cp} and \frac{\mu_b}{k_b} < \frac{\mu_f}{k_f} \end{cases}$ $Re_b = \frac{Md}{\mu_b}$, $Re_f = \frac{Md}{\mu_f}$, $h = \frac{Nuk_f}{d}$ f_f is given by Filonenko [93] equation at mean film temperature.
Huai et al. [35,36]	(D = 1.31 mm, L = 500 mm)	$Nu = 2.2126x10^{-2}Re_b^{0.8}Pr_b^{0.3}(\frac{\rho_b}{\rho_w})^{-1.4652}(\frac{\overline{Cp}}{Cp_w})^{0.0832}$ Where, $\overline{Cp} = \frac{H_b - H_w}{T_b - T_w}$ and Cp_w and ρ_w are evaluated on wall temperature, ρ_b is calculated on bulk mean temperature of sCO_2
Krasnoshchekov and Protopopov [57,60]	(D = 4.08 mm, L = 208 mm)	$\frac{Nu}{Nu'_b} = \left(\frac{\rho_w}{\rho_b}\right)^{0.3}\left(\frac{\overline{Cp}}{Cp_w}\right)^n$ $n = 0.4$ for $T_b \leq T_w \leq T_{pc}$ and $1.2T_{pc} \leq T_b < T_w$ $n = 1.2$ for $1.2T_{pc} \leq T_b \leq T_w$ $n = 0.4 + 0.2(\frac{T_w}{T_{pc}} - 1)$ for $T_b \leq T_{pc} \leq T_w$ $n = 0.4 + 0.2\left(\frac{T_w}{T_{pc}}-1\right)[1 - 5\left(\frac{T_b}{T_{pc}}-1\right)]$ for $T_{pc} \leq T_b \leq 1.2T_{pc}$ Nu'_b is expressed by the correlation reported by Petukhov [92] evaluated at mean bulk temperature.
Literature	**Tube Geometry**	**Correlation**
Bruch et al. [66]	(D = 6 mm, L = 750 mm)	$\frac{Nu}{Nu_{FC}} = 1 - 75\left(\frac{Gr}{Re_b^{2.7}}\right)^{0.46}$ When, $\frac{Gr}{Re_b^{2.7}} < 4.2x10^{-5}$ $\frac{Nu}{Nu_{FC}} = 13.5\left(\frac{Gr}{Re_b^{2.7}}\right)^{0.46}$ When, $\frac{Gr}{Re_b^{2.7}} > 4.2x10^{-5}$ Where Nu_{FC} is the average Nusselt number for pure forced convection expressed by the following equation $Nu_{FC} = 0.0183Re_b^{0.82}\overline{Pr_b}^{0.5}\left(\frac{\rho_b}{\rho_w}\right)^{-0.3}$ Where, $Gr = \frac{(\rho_w - \rho_b)\rho_b g d^3}{\mu_b^2}$ $\overline{Pr} = \frac{\overline{Cp}}{h_{out} - h_{in}}\int_{hin}^{hout}\frac{\mu(h)}{k(h)}dh$
Liao and Zhao [24,67]	(D = 0.7, 1.4 and 2.16 mm, L = 110 mm)	$Nu = 0.128Re_w^{0.8}Pr_w^{0.3}\left(\frac{Gr}{Re_b^2}\right)^{0.205}\left(\frac{\rho_b}{\rho_w}\right)^{0.437}\left(\frac{\overline{Cp}}{Cp_w}\right)^{0.411}$

(continued on next page)

Table 5 (*continued*)

Literature	Tube Geometry	Correlation
Gupta et al. [69]	(D = 8 mm, L = 2208 mm)	$Nu_w = 0.0038Re_w^{0.957}\,\overline{Pr_w}^{-0.139}\left(\frac{\rho_w}{\rho_b}\right)^{0.836}\left(\frac{k_w}{k_b}\right)^{-0.754}\left(\frac{\mu_w}{\mu_b}\right)^{-0.222}$ $Nu_b = 0.0094Re_b^{0.892}\,\overline{Pr_b}^{-0.141}\left(\frac{\rho_w}{\rho_b}\right)^{0.926}\left(\frac{k_w}{k_b}\right)^{0.216}\left(\frac{\mu_w}{\mu_b}\right)^{-1.128}$ $Nu_f = 0.0043Re_f^{0.935}\left(\frac{\rho_w}{\rho_b}\right)^{0.572}\left(\frac{k_w}{k_b}\right)^{-0.524}$
Kruizenga et al. [81]	(D = 1.9 mm and L = 500 mm)	$Nu = 0.0183Re_b^{0.82}\,Pr_b^{0.5}\left(\frac{\rho_w}{\rho_b}\right)^{0.3}\left(\frac{\overline{C_p}}{C_{pb}}\right)^{n}\left(\frac{C_{pb}}{C_{p-IG}}\right)^{-0.19}$ Where C_{p-IG} specific heat of carbon dioxide as an ideal gas evaluated at T_{pc} and value of n is given by Jackson and Hall [78] correlation.
Jackson and Hall [78]	(D = 1.6–20 mm)s	$Nu = 0.0183Re_b^{0.82}\,Pr_b^{0.5}\left(\frac{\rho_w}{\rho_b}\right)^{0.3}\left(\frac{\overline{C_p}}{C_{pb}}\right)^{n}$ $n = 0.4$ for $T_b < T_w < T_{pc}$ and $1.2T_{pc} < T_b < T_w$ $n = 0.4 + 0.2\left(\frac{T_w}{T_{pc}} - 1\right)$ for $T_b < T_{pc} < T_w$ $n = 0.4 + 0.2\left(\frac{T_w}{T_{pc}}-1\right)\left[1 - 5\left(\frac{T_b}{T_{pc}}-1\right)\right]$ for $T_{pc} < T_b < 1.2T_{pc}$ and $T_b < T_w$
Petrov and Popov [82]	Not mentioned	$\frac{Nu}{Nu_{ow}} = \left(1 - m\frac{q}{G}\right)\left(\frac{\overline{C_p}}{C_{pw}}\right)^{n}$ $n = 0.66 - K\frac{q}{G}$, when $\frac{\overline{C_p}}{C_{pw}} \le 1$ and $n = 0.9 - K\frac{q}{G}$, when $\frac{\overline{C_p}}{C_{pw}} > 1$ $\frac{f}{f_w} = \frac{\rho_w}{\rho_b}\left(\frac{\mu_w}{\mu_b}\right)^{S}$ $S = 0.023\left(\frac{q}{G}\right)^{0.42}$ m = 0.001 kg/J K = 4×10^{-4} kg/J Nu_{ow} is the Nusselt number given by Petukhov [92] correlation. $Nu_{ow} = \frac{\left(\frac{f}{8}\right)Re_w Pr_w}{12.7\left(\frac{f}{8}\right)^{0.5}\left(Pr_w^{\frac{2}{3}}-1\right)+1.07}$ Friction factor equation is calculated by Filonenko [93] equation.
Fang et al. [77]	Not mentioned	$Nu = \frac{\left(\frac{f_w}{8}\right)(Re_w - 1000)Pr_w}{A + 12.7\left(\frac{f_w}{8}\right)^{0.5}\left(Pr_w^{\frac{2}{3}}-1\right)}\left(1 - 0.001\frac{q}{G}\right)\left(\frac{\overline{C_p}}{C_{pw}}\right)^{n}$ $f_w = [0.79\log(Re_w) - 1.64]^{-2}$ $A = 1 + 7 \times 10^{-8}Re_w$ for $Re_w < 10^6$ and $A = 1.07$ for $Re_w > 10^6$ $n = 0.66 + 4x10^{-4}\left(\frac{q}{G}\right)$ if $\frac{\overline{C_p}}{C_{pw}} \le 1$ $n = 0.9 + 4x10^{-4}\left(\frac{q}{G}\right)$ if $\frac{\overline{C_p}}{C_{pw}} > 1$
Petrov and Popov [87]	Not mentioned	$Nu = \frac{\left(\frac{f}{8}\right)Re_b\overline{Pr}}{1.07 + 12.7\left(\frac{f}{8}\right)^{0.5}\left[\overline{Pr}^{\frac{2}{3}}\left(\frac{\rho_w}{\rho_b}\right)^{0.5}\left(1 - 0.9\sqrt{\frac{\lvert f_i\rvert}{f}}\right) - \left(1 - \sqrt{\frac{\lvert f_i\rvert}{f}}\right)\right]}$ $\frac{f}{f_b} = \left(\frac{\mu_w}{\mu_b}\right)^{0.25} + 0.17\left(\frac{\rho_w}{\rho_b}\right)^{1/3}\frac{\lvert f_i\rvert}{f_b}$ $f_i = -\frac{4d}{\rho_b}\frac{d\rho_b}{dz}$ and $\overline{Pr} = \frac{\mu_b\overline{C_p}}{k_b}$ f_b is given by Filonenko [93] equation measured at mean bulk temperature.
Kirillov et al. [89]	Not mentioned	$k^* = \left(1 - \frac{\rho_w}{\rho_b}\right)\frac{Gr}{Re_b^2}$ For $k^* < 0.01$, the heat transfer correlation is expressed by $Nu = Nu_o\left(\frac{\rho_w}{\rho_b}\right)^{0.3}\left(\frac{\overline{C_p}}{C_{pb}}\right)^{n}$ $k^* > 0.01$, the heat transfer correlation is expressed by $Nu = Nu_o\left(\frac{\rho_w}{\rho_b}\right)^{0.3}\left(\frac{\overline{C_p}}{C_{pb}}\right)^{n}\varphi(k^*)$ $Nu_o = \frac{\left(\frac{f_b}{8}\right)Re_b\overline{Pr_b}}{\left(\frac{900}{Re_b}\right) + 4.5(f_b)^{0.5}\left(\overline{Pr_b}^{2/3} - 1\right)}$ The correlation is valid for $\overline{Pr_b} = 0.1 - 200$ and $Re_b = 4x10^3 - 5000x10^3$. The value of $\varphi(k^*)$ is given by the following equation

(*continued on next page*)

Table 5 (*continued*)

Literature	Tube Geometry	Correlation
		$\varphi(k^*) = 0.79782686 - 1.6459037lnk^* - 2.7547316(lnk^*)^2 - 1.7422714(lnk^*)^3 - 0.54805506(lnk^*)^4 - 0.086914323(lnk^*)^5 - 0.0055187343(lnk^*)^6$ $n = 0.4$ for $\frac{T_w}{T_{pc}}<1$ and $\frac{T_b}{T_{pc}}>1.2$ $n = 0.22 + 0.18\frac{T_w}{T_{pc}}$ for $\frac{T_w}{T_{pc}}>1$ and $\frac{T_b}{T_{pc}}<1.2$ $n = 0.9\frac{T_b}{T_{pc}}\left(1-\frac{T_w}{T_{pc}}\right)+1.08\frac{T_w}{T_{pc}} - 0.68$ for $\frac{T_w}{T_{pc}}>1$ and $1<\frac{T_b}{T_{pc}}<1.2$
Li et al. [90]	(D = 1.16 mm and L = 500 mm)	$Nu = 0.023Re_b^{0.8}Pr_b^{0.4}\left(\frac{\rho_w}{\rho_b}\right)^{0.3}\left(\frac{\overline{C_p}}{C_{pb}}\right)^n$ Here, value of n is given by Jackson and Hall [78] correlation.
Kuang et al. [91]	(D = 0.79 mm)	$Nu = 0.001546Re_b^{1.054}Pr_b^{0.653}\left(\frac{\rho_w}{\rho_b}\right)^{0.367}\left(\frac{\overline{C_p}}{C_{pb}}\right)^{0.4}$
Mokry et al. [95]	Not mentioned	$Nu = 0.0121Re_b^{0.86}\overline{Pr}_b^{0.23}\left(\frac{\rho_w}{\rho_b}\right)^{0.59}$
Ghajar and Asadi [96]	Not mentioned	$Nu = 0.025Re_b^{0.8}Pr_b^{0.417}\left(\frac{\rho_w}{\rho_b}\right)^{0.32}\left(\frac{C_{p,i}}{C_{pw}}\right)^n$ Where value of n is given by Jackson and Hall [78] correlation.

32 °C, the mass flux 0.003–0.3 kg/min, and the uniform heat flux 100–800 W/m^2. In the vicinity of pseudocritical region, due to sharpe decrease of density and sharp rise of specific heat capacity, the convective heat transfer coefficient augmented with an increase mass flux and wall heat flux. The velocity and temperature profiles were not fully developed confirmed from the numerical simulation which caused the earlier flow transition and further improvement of the heat transfer coefficient. Fang et al. [77], Zhou and Krishnan [85] and Bae et al. [86] also performed comparison of experimental dataset with numerically predicted values for forced convection heat transfer of sCO_2 under turbulent flow condition in circular pipe geometries.

6. sCO_2 heat transfer and friction factor correlation

The conventional correlations of turbulent forced convection for constant property fluids failed to predict the heat transfer mechanism in the vicinity of the critical condition. The nonlinear variations of thermodynamic and transport properties at the pseudocritical region demand new heat transfer correlation to take account of the drastic variation of properties. In order to incorporate the effect of temperature dependent thermodynamic properties of sCO_2 near the critical region, researchers employed two methods for the formulation of heat transfer correlation. In reference temperature method, all the thermo-physical properties calculated at the mean bulk fluid temperature, the mean wall temperature or the mean of bulk and wall temperature. The other widely used method called property ratio method, where the ratio of properties calculated at bulk fluid and wall temperature are included in correlation. Mainly the properties such as isobaric specific heat and density which exhibit extreme rapid variation near the pseudocritical temperature incorporated in the turbulent forced convection heat transfer correlation.

Yoon et al. [31] recommended a heat transfer correlation by employing property ratio method for tube diameter of 7.73 mm and operating pressure 7.5–8.8 MPa. The authors [31] then reduced the complexity in the equation and proposed a heat transfer correlation in simple form separating the regimes above and below the pseudo-critical temperature of the supercritical carbon dioxide. Bruch et al. [66] experimented with super critical carbon dioxide cooled in a plain tube and proposed a correlation, which takes into account of the influence of buoyancy. Petrov and Popov [82] developed correlation for local Nusselt number applicable for in tube cooling for sCO_2. Later, Petrov and Popov [87] developed correlation for heat transfer in the form of average Nusselt Number for cooling in a horizontal tube for a wide range of data using the reference temperature method. Their proposed correlation has the limits of applicability: $3.1 \times 10^4 < Re_b < 8 \times 10^5$, $1.4 \times 10^4 < Re_w < 7.9 \times 10^5$ and $-350 < q/G <$ -29 J/kg. Pitla et al. [29,32] performed experimental and modelling study for turbulent forced convection heat transfer of sCO_2 cooled in a circular tube and proposed a new correlation by modifying the Gnielinski [88] correlation. Baskov et al. [56] proposed correlation using property ratio method for cooling of supercritical fluids with horizontal macro tubes. Kirillov et al. [89]demonstrated the role of free convection for flow through a circular channel near critical point by defining a new parameter. Li et al. [90] developed heat transfer correlation with an aid of property ratio method for both heating and cooling modes with sCO_2 flowing through a horizontal circular tube. A correlation was proposed where the probability density function (PDF)-based time-averaged properties were included in the equation in order to reflect the change of thermo-physical properties near the critical condition of CO_2. Besides these, Liu et al. [1], Oh and Son [25], Son and park [30], Dang and Hihara [33], Huai et al. [35,36], Liao and Zhao [24,67], Gupta et al. [69], Fang et al. [77], Kuang et al. [91] and Fang and Xu [19] also developed heat transfer correlations in terms of Nusselt number applicable for supercritical CO_2 in horizontal tube configuration, shown in tabular from in Table 5. Krasnoshchekov et al. [26] proposed a correlation for average Nusselt number.

$$\frac{Nu}{Nu_w} = \left(\frac{\rho_w}{\rho_b}\right)^n\left(\frac{\overline{C_p}}{C_{pw}}\right)^m \tag{2}$$

$$m = B\left(\frac{\overline{C_p}}{C_{pw}}\right)^l \tag{3}$$

Nu_w is given by the Petukhov [92] correlation and the friction factor equation is given by Filonenko [93]. The correlation is valid for the ranges: $9 \times 10^4 < Re_b < 3.2 \times 10^5$ and $6.3 \times 10^5 < Re_w < 2.9 \times 10^5$. Values for n, B and l are given for different operating inlet pressure in Table 3.

Baskov et al. [56] developed the heat transfer correlation applicable for cooling in horizontal macro tubes.

$$\frac{Nu}{Nu_w} = \left(\frac{\rho_w}{\rho_b}\right)^n\left(\frac{\overline{C_p}}{C_{pw}}\right)^m \tag{4}$$

Nu_w is expressed by the Petukhov [92] correlation and the friction factor equation is given by Filonenko [93] by wall temperature approach. Here m = 1.4 and n = 0.15 for $T_b/T_{pc} \le 1$. For $T_b/T_{pc} > 1$, m and n values are given in Table 4.

To the best of our knowledge, most of the correlations for supercritical CO_2 have been formulated for heat transfer. Friction factor plays an essential role in the fluid flow behaviour mechanism in terms of shear stress development near the wall boundary. Most of the researchers employed the friction factor equations for supercritical CO_2 in various applications available in the literature. Table 6, shows the list of friction factor equations applicable for supercritical CO_2 under heating and cooling condition.

Yoon et al. [31] performed experimentation with sCO_2 cooled in a horizontal circular tube of 7.73 mm of inner diameter. The experimental values of convective heat transfer coefficient were compared with Krasnoshchekov et al. [26], Pitla et al. [29,32], Baskov et al. [56] and Petrov and Popov [82]. From Fig. 11, Pitla et al. [29,32] correlation was unable to predict the value of heat transfer coefficient for all range of bulk temperature. Other correlations showed reasonable agreement with the experimental findings except near the critical region. Based on their experiment study, Yoon et al. [31] proposed a heat transfer correlation in terms of average Nusselt number by incorporating the effect of transport properties of sCO_2 near the critical region. The proposed correlation was developed for region above and below the pseudocritical temperature. This is the only correlation available in literature based on purely bulk temperature approach. Comparison of correlation with experimental results was also performed by Dang and Hihara [33] for in tube gas cooling process in a circular tube with horizontal orientation, as shown in Fig. 12. The value of forced convective heat transfer coefficient α, with the bulk fluid temperature was compared with Yoon et al. [31], Liao and Zhao [24], Pitla et al. [29,32], Petrov and Popov [82] and Gnielinski [88] correlations. This experimental study conducted for a 6 mm diameter circular tube under the heat flux of 24 kW/m^2 and the mass flow rate of 200 kg/m^2 s. Near the pseudocritical region, all the correlations were failed to predict the value of heat transfer coefficient. The proposed correlation was a modified form of Gnielinski [88] correlation. The

Table 6
Review of friction factor equations applicable for sCO_2.

Literature	Equation
Petrov and Popov [82]	$f = f_w \frac{\rho_w}{\rho_b}(\frac{\mu_w}{\mu_b})^s$ $s = 0.023(\frac{q}{G})^{0.42}$ $f_w = [1.82\log(Re_w) - 1.64]^{-2}$
Fang and Xu [19]	$f = f_{noniso} - 1.36(\frac{\mu_w}{\mu_b})^{-1.92} f_{ac}$ $f_{ac} = \frac{D}{L}(\rho_{b,out} - \rho_{b,in})(\frac{1}{\rho_{b,out}} - \frac{1}{\rho_{b,in}})$ The non-isothermal friction factor is expressed by $f_{noniso} = f_{iso,b}(\frac{\mu_w}{\mu_b})^{-0.49(\frac{\rho_f}{\rho_{pc}})^{1.31}}$ The isothermal friction factor is expressed by $f_{iso,b} = 1.613[\ln\left(0.234\left(\frac{\varepsilon}{D}\right)^{1.1007} - \frac{60.525}{Re_b^{1.1105}} + \frac{56.291}{Re_b^{1.0712}}\right)]^{-2}$
Filonenko [93]	$f = [1.82\log(Re_b) - 1.64]^{-2}$
Colebrook and White [97]	$f^{-0.5} = -2\log(\frac{\frac{\varepsilon}{D}}{3.7} + \frac{2.51}{Re_b\sqrt{f}})$
Swanee and Jain [98]	$f = \frac{0.25}{[\left(\frac{\frac{\varepsilon}{D}}{3.7} + \frac{2.51}{Re_b\sqrt{f}}\right)]^2}$
Churchill [99]	$f = 8\{(\frac{8}{Re_b})^{12} + [2.457\ln(\frac{1}{(\frac{7}{Re_b})^{0.9} + 0.27\frac{\varepsilon}{D}})^{16} + (\frac{37530}{Re_b})^{16}]^{-1.5}\}^{\frac{1}{12}}$
Ozışık [100]	$f^{-0.5} = -2\log(Re_b\sqrt{f}) - 0.8$
Haaland [101]	$f = 0.3086[\log\left\{\frac{6.9}{Re_b} + \left(\frac{\frac{\varepsilon}{D}}{3.7}\right)^{1.11}\right\}]^{-2}$ for $\frac{\varepsilon}{D} > 10^{-4}$ $f = 2.7778[\log\left\{(\frac{7.7}{Re_b})^3 + \left(\frac{\frac{\varepsilon}{D}}{3.75}\right)^{3.33}\right\}]^{-2}$ for $\frac{\varepsilon}{D} < 10^{-4}$
Nikuradse [102]	$\frac{1}{f^{-0.5}} = 0.86\ln(Re_b^{0.5}) - 0.8$
Benedict [103]	$f = 0.25[(\frac{\frac{\varepsilon}{D}}{3.7}) + \frac{5.74}{Re_b^{0.9}}]^{-2}$

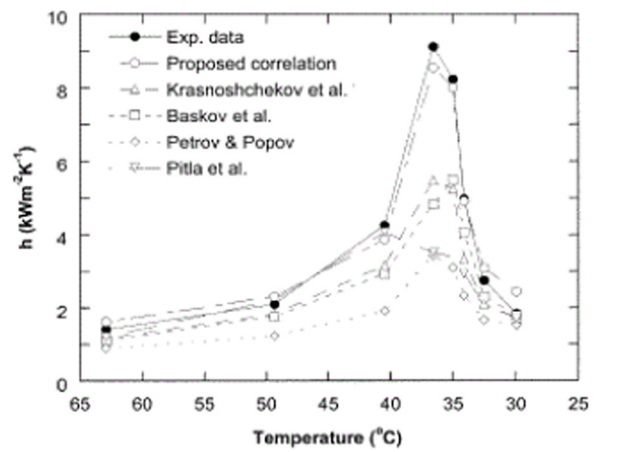

Fig. 11. Comparison of correlation with experimental findings (Yoon et al. [31]).

correlation was reported with the use of reference temperature method and the accuracy was within the limit of 20%. Mean error and root mean square (RMS) error for various correlations were calculated by Surendran et al. [20]. Among all the correlations, Swenson et al. [94] proved to be more accurate than any other existing correlations. Error analysis also carried out by Gupta et al. [22] for the existing sCO_2 heat transfer correlations. Fang and Xu [19] compared the performance of different sCO_2 heat transfer correlations in terms of mean absolute relative deviation (MARD) values.

From the literature, it is concluded that each correlation was developed based on experimental studies; therefore, each correlation has its own range of limits. It should be noted that various heat transfer correlations deviate from each other due to several reasons. Each correlation was developed based on experimental study. Therefore, the same correlation when compared with different experimental dataset, it showed significant deviation due to the change of the range of investigated parameters. Furthermore, some earlier correlations were developed without considering the rapid change of physical properties of the working fluid. The newly developed correlations which take account of the change of properties especially specific heat, density and viscosity are more reliable and consistent. However, during heating of sCO_2, the correlation failed to predict the deteriorated heat transfer. The correlation which was proposed for cooling of sCO_2, does not guarantee for better prediction of heat transfer coefficient while applied for heating application and vice versa. On top of that, the influence of buoyancy significantly affects the heat transfer performance. Some correlations were developed without taking account of buoyant force. So, in general, no single correlation can cover the whole range of

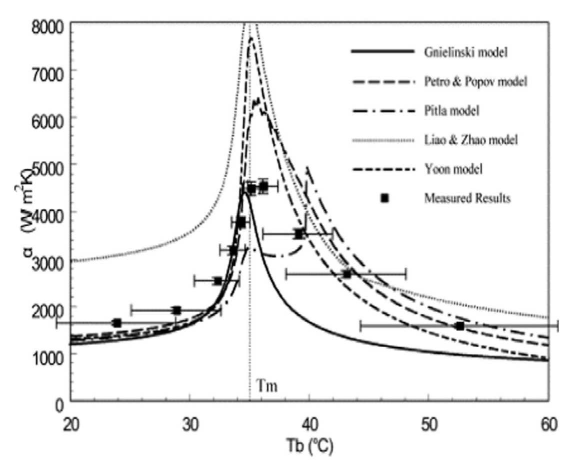

Fig. 12. Correlation study by Dang and Hihara et al. [33].

Table 7
Review of heat transfer correlations applicable for supercritical water.

Literature	Correlation	Applicability
Swenson [94]	$Nu_w = 0.00459 Re_w^{0.923}\,\overline{Pr}_w^{0.613}\left(\frac{\rho_w}{\rho_b}\right)^{0.231}$ where, $\overline{Pr}_w = \frac{\mu_w \overline{Cp}}{k_w}$	P = 22.8–41.4 MPa, G = 542–2150 kg/m^2 s T_b = 75–576 °C
Gupta et al. [104]	$Nu_w = 0.0033 Re_w^{0.94}\,\overline{Pr}_w^{0.76}\left(\frac{\rho_w}{\rho_b}\right)^{0.156}\left(\frac{\mu_w}{\mu_b}\right)^{0.4}$	Supercritical ranges
Bringer and Smith [105]	$Nu = 0.0266 Re_x^{0.77}\,Pr_w^{0.55}$ Re_x is the Reynolds number evaluated at temperature T_x.	$T_x = T_b$ if $\frac{(T_{pc}-T_b)}{(T_w-T_b)}<0$ $T_x = T_{pc}$, if $0\le\frac{(T_{pc}-T_b)}{(T_w-T_b)}\le 1$ $T_x = T_w$ if $\frac{(T_{pc}-T_b)}{(T_w-T_b)}>1$
Shitsman [106]	$Nu = 0.023 Re_b^{0.8}\,Pr_{min}^{0.8}$	Supercritical ranges
Bishop et al. [107]	$Nu_x = 0.0069 Re_x^{0.9}\,\overline{Pr}_x^{0.66}\left(\frac{\rho_w}{\rho_b}\right)_x^{0.43}\left(1 + 2.4\frac{D}{x}\right)$ $\overline{C_p} = \frac{H_b - H_w}{T_b - T_w}$, $\overline{Pr}_x = \frac{\mu_b \overline{Cp}}{k_b}$	P = 22.8–27.6 MPa, G = 282–527 kg/m^{2}s T_b = 75–576 °C q = 310–3460 kW/m^2
Ornatsky et al. [108]	$Nu = 0.023 Re_b^{0.8}\,Pr_{min}^{0.8}\left(\frac{\rho_w}{\rho_b}\right)^{0.3}$ Where Pr_{min} is the minimum value of Pr_b or Pr_w	Supercritical ranges
Yamagata et al. [109]	$Nu = 0.0135 Re_b^{0.85}\,Pr_{min}^{0.8}\,F_c$ Where $F_c = 1$ for $E > 1$ and $E = \frac{(T_{pc}-T_b)}{(T_w-T_b)}$ $F_c = 0.64 Pr_{pc}^{-0.05}\left(\frac{\overline{Cp}}{C_{pb}}\right)^{n1}$ for $0 \le E \le 1$, $F_c = \left(\frac{\overline{Cp}}{C_{pb}}\right)^{n2}$ *for* $E < 0$ $n1 = -0.77\left(1+\frac{1}{Pr_{pc}}\right) + 1.49$, $n2 = -1.44\left(1+\frac{1}{Pr_{pc}}\right) - 0.53$	P = 22.6–29.4 MPa G = 310–1830 kg/m^2 s
Yaskin et al. [110]	$\frac{Nu}{Nu_o} = \left[1 - 0.2\frac{Nu}{Nu_o}\beta(T_w - T_b)\right]^2$ Where, $Nu_o = 0.0243 Re_b^{0.8}\,Pr_b^{0.4}$	Supercritical ranges
Yeroshenko et al. [111]	$Nu = 0.0243 Re_b^{0.8}\,Pr_b^{0.4}\left[\frac{2}{\{0.8 + 0.8\beta(T_w - T_b)\}^{0.5} + 1.447}\right]^2$ Here, $F = \left(\frac{\overline{Cp}}{C_{pb}}\right)^{0.28}$ for $\overline{C_p} > C_{pb}$ and $F = 1$ for $\overline{C_p} \le C_{pb}$ When $[1 + \beta(T_w - T_b)]>2$ the correlation is reduced to $Nu = 0.0243 Re_b^{0.8}\,Pr_b^{0.4}\left[\frac{2}{\{0.8 + 0.8\beta(T_w - T_b)\}^{0.5} + 1.447}\right]^2$	Supercritical ranges
Kitoh et al. [112]	$Nu = 0.0153 Re_b^{0.85}\,Pr_b^{m}$ $m = \left(0.69-\left(\frac{8100}{q}\right) + F_c q\right.$ and $q = 200G^{1.2}$ $F_c = 2.9x10^{-8}+\left(\frac{0.11}{q}\right)$ for $0\le H_b\le$ 1500 kJ/kg $F_c = -8.7x10^{-8}-\left(\frac{0.65}{q}\right)$ for $1500\le H_b\le$ 3300 kJ/kg $F_c = -9.7x10^{-7}+\left(\frac{1.3}{q}\right)$ for $3300\le H_b\le$ 4000 kJ/kg	Supercritical ranges
Domin [113]	$Nu_b = 0.1 Re_b^{0.66}\,\overline{Pr}_b^{1.2}$ for $Nu_b = 0.036 Re_b^{0.8}\,\overline{Pr}_b^{0.4}\left(\frac{\mu_w}{\mu_b}\right)$, when $T_w > 350$ °C	P = 23.3–26.3 MPa G = 580–4650 kg/m^2 s T_w = 250–350 °C
Kondrat'ev [114]	$Nu_b = 0.020 Re_b^{0.8}$	P = 25.2–32 MPa T_w = 130–600 °C
Gorban et al. [115]	$Nu_b = 0.0059 Re_b^{0.9}\,Pr_b^{-0.12}$	Supercritical ranges
Griem [116]	$Nu = 0.0169 Re_b^{0.8356}\,Pr_b^{0.432}\varphi$ $\varphi = 0.82$, if $0\le H_b\le$ 1540 kJ/kg $\varphi = 0.82 + 0.18\frac{H_b - 1540}{200}$, if $1540\le H_b\le$ 1740 kJ/kg $\varphi = 1.0$, if $H_b\ge$ 1540 kJ/kg	P = 22.0–27.0 MPa G = 300–2500 kg/m^{2}s q = 200–700 kW/m^2

operating parameters and all correlations have some limitations. For practical implementation of sCO_2 correlation, it is highly recommended to check the limits of applicability and further experimental investigations are essential to predict the heat transfer and flow behaviour in the vicinity of pseudocritical region due to drastic property variation. The new correlation must take account of the influence of buoyancy and should be applicable for full range of operating conditions. Since heat transfer deterioration is still a complex phenomenon during heating application, the new correlation applicable for sCO_2 heating must take account of deteriorated heat transfer.

Supercritical fluids have successful implementation in power engineering, supercritical extraction and supercritical fluid chromatography in chemical engineering, cooling of superconducting electromagnets in cryogenics engineering and refrigeration technologies. Table 7 shows some of the earlier researches with supercritical water and the proposed correlations with their range of applicability. For comparison of heat transfer mechanism between supercritical water and sCO_2, the table gives some reviews on heat transfer correlations [94] for supercritical water. This table provides an additional information for the researchers who are interested in dealing with supercritical water in supercritical pressure water-cooled reactor, fossil power plants, Biofuel Production, Petrochemical Applications, supercritical water oxidation and chemical synthesis like organic reactions and organometallic reactions.

7. Conclusion

The environmentally benign properties of CO_2 provide full safety and natural solution. Therefore, it has becoming one of the promising refrigerants successfully implemented in many process and chemical industries. The operating parameters such as mass velocity, heat flux, pressure and temperature have significant influence on the convective heat transfer coefficient under both heating and cooling modes. The heat transfer performance increases with increased Reynolds number and with decreased inlet pressure of sCO_2 close to critical condition due to extreme variation of thermo-physical properties e.g. the peak of specific heat at pseudocritical temperature. The pressure drop decreases when the operating pressure is increased due to less dominant property variation further away from the critical point. Under cooling condition, the heat transfer rate increases with reduced tube diameter due to the increase of surface area, whereas under heating condition, heat transfer shows the opposite trend. Therefore, instead of mass velocity, the effect of tube diameter on the heat transfer mechanism should be evaluated based on same Reynolds number.

Heat transfer deterioration is found to be associated under heating of sCO_2 in various flow configuration. The wall temperature profile significantly affects the heat transfer rate, especially when the wall temperature approaches the pseudocritical temperature and the bulk temperature still below the pseudocritical temperature. The earlier peak of the wall temperature provides distortion of shear stress near the wall boundary and causes heat transfer deterioration due to reduction of turbulent production. Fundamental understanding of the complex phenomenon of heat transfer deterioration of supercritical fluids under heating condition is still a continuing research topic for many researchers. A comprehensive quantitative analysis is essential to investigate the exact flow condition for which heat transfer deterioration take place during heating of supercritical fluids.

In this work, we present a review of heat transfer correlations with range of application and friction factor equations suitable for supercritical CO_2. Each correlation based on experimental studies has its own limits of applicability. The tube diameter, the operating mass velocity and the heat flux significantly influence the effectiveness of heat transfer. Researchers have performed experimentation with sCO_2 under various operating conditions. This is one of the possible reasons for why not all of the correlations can properly predict the convective heat transfer coefficient, especially near the pseudocritical region. Further experimental and numerical studies are needed to develop a new heat transfer correlation applicable for sCO_2 for full range operating parameters involving micro to macro tube size, mass flux, heat flux and operating temperature and pressure. During heating of sCO_2, the new heat transfer correlation could be proposed for normal heat transfer region and deteriorated heat transfer region.

Acknowledgement

This research was conducted as a part of the Australia Solar Thermal Research Initiative (ASTRI), a project supported by Australia government through the Australia Renewable Energy Agency (ARENA). The first author, M. Monjurul Ehsan would also like to acknowledge University of Queensland (UQ) for providing Research Training Program (RTP) and Australian Postgraduate Award (APA) scholarships.

References

[1] Liu Z-B, He Y-L, Yang Y-F, Fei J-Y. Experimental study on heat transfer and pressure drop of supercritical CO 2 cooled in a large tube. Appl Therm Eng 2014;70(1):307–15.

[2] Oh H, Hong J. Condensing heat transfer characteristics of alternative refrigerants in small diameter tubes. J SAREK 1999;28(5):396–402.

[3] Torikoshi K. Heat transfer and pressure drop characteristics of R 134a, R 32 and a mixture of R 32/R 134a inside a horizontal tube. ASHRAE Trans 1993;99:90–6.

[4] Tandon T, Varma H, Gupta C. Generalized correlation for condensation of binary mixtures inside a horizontal tube. Int J Refrig 1986;9(3):134–6.

[5] Son C-H, Choe Y-S, Kim G-S. The condensation pressure drop of alternative refrigerants for R-22 in small diameter tubes. Trans Korean Soc Mech Eng B 2001;25(9):1245–52.

[6] Cheng X, Schulenberg T. Heat transfer at supercritical pressures: literature review and application to an HPLWR. FZKA 2001.

[7] Ito T, Takata Y, Kasao D, Yamaguchi M, Hara T. Forced convection heat transfer to supercritical helium flowing in a vertical straight circular tube. AIChE Symp Ser; 82; 1986. p. 86–91.

[8] Valyuzhin M, Kuznetsov YV. Transfer of heat to supercritical helium in the inlet region of a circular tube under highly nonisothermal conditions. Heat Transf Sov Res 1986;18(6):97–103.

[9] Dziedzic W, Jones S, Gould D, Petley D. An analytical comparison of convective heat transfer correlations insupercritical hydrogen. In: Proceedings of the 26th thermophysics conference, p. 1382.

[10] Lorentzen G. The use of natural refrigerants: a complete solution to the CFC/HCFC predicament. Int J Refrig 1995;18(3):190–7.

[11] Halozan H, Rieberer R. CO_2 as refrigerant-possible applications. Sci Tech Froid 2001:89–96.

[12] Byrne P, Miriel J, Lenat Y. Design and simulation of a heat pump for simultaneous heating and cooling using HFC or CO 2 as a working fluid. Int J Refrig 2009;32(7):1711–23.

[13] Lorentzen G, Pettersen J. A new, efficient and environmentally benign system for car air-conditioning. Int J Refrig 1993;16(1):4–12.

[14] Dubey AM, Kumar S, Agrawal GD. Thermodynamic analysis of a transcritical CO 2/propylene (R744–R1270) cascade system for cooling and heating applications. Energy Convers Manag 2014;86:774–83.

[15] Pitla SS, Robinson DM, Groll EA, Ramadhyani S. Heat transfer from supercritical carbon dioxide in tube flow: a critical review. HVAC&R Res 1998;4(3):281–301.

[16] Pioro IL, Khartabil HF, Duffey RB. Heat transfer to supercritical fluids flowing in channels—empirical correlations (survey). Nucl Eng Des 2004;230(1):69–91.

[17] Duffey RB, Pioro IL. Experimental heat transfer of supercritical carbon dioxide flowing inside channels (survey). Nucl Eng Des 2005;235(8):913–24.

[18] Cheng L, Ribatski G, Thome JR. Analysis of supercritical CO 2 cooling in macro- and micro-channels. Int J Refrig 2008;31(8):1301–16.

[19] Fang X, Xu Y. Modified heat transfer equation for in-tube supercritical CO 2 cooling. Appl Therm Eng 2011;31(14):3036–42.

[20] Surendran P, Gupta S, Preda T, Pioro I. Comparison of existing supercrtical carbon dioxide heat transer correlations for horizontal and vertical bare tubes. In: Proceedings of the 20th international conference on nuclear engineering and the ASME power conference. American Society of Mechanical Engineers; 2012. p. 335–42.

[21] Lin W, Du Z, Gu A. Analysis on heat transfer correlations of supercritical CO_2 cooled in horizontal circular tubes. Heat Mass Transf 2012;48(4):705–11.

[22] Cheng L. Evaluation of correlations for supercritical CO2 cooling convective heat transfer and pressure drop in macro-and micro-scale tubes. Int J Microscale Nanoscale Therm Fluid Transp Phenom; 5(2); 2014. p. 113.

[23] Cheng L. Evaluation of correlations for supercritical CO_2 cooling convective heat transfer and pressure drop in macro-and micro-scale tubes. Int J Microsc Nanoscale Therm Fluid Transp Phenom 2014;5(2):113.

[24] Liao S, Zhao T. Measurements of heat transfer coefficients from supercritical carbon dioxide flowing in horizontal mini/micro channels. Trans-Am Soc Mech Eng J Heat Transf 2002;124(3):413–20.

[25] Oh H-K, Son C-H. New correlation to predict the heat transfer coefficient in-tube cooling of supercritical CO 2 in horizontal macro-tubes. Exp Therm Fluid Sci 2010;34(8):1230–41.

[26] Krasnoshchekov E, Kuraeva I, Protopopov V. Local heat transfer of carbon dioxide at supercritical pressure under cooling conditions. High Temp 1969;7(5):856.

[27] Krasnoshchekov E, Ia P, Silin V, Vs P. Some results of an experimental investigation of heat-transfer to carbon-dioxide at supercritical pressure and temperature heads of up to 0 °C, vol. 9. Maik Nauka/Interperiodica/Springer, 233 Spring St, New York, NY 10013-1578 USA; 1972. p. 992-+.

[28] Ankudinov VB, Kurganov VA. Intensification of a declined heat transfer in heated tubes at supercritical pressures. Teplofiz Vysok Temp 1981;19(6):1208–12.

[29] Pitla SS, Groll EA, Ramadhyani S. Convective heat transfer from in-tube cooling of turbulent supercritical carbon dioxide: part 2—experimental data and numerical predictions. HVAC&R Res 2001;7(4):367–82.

[30] Son C-H, Park S-J. An experimental study on heat transfer and pressure drop characteristics of carbon dioxide during gas cooling process in a horizontal tube. Int J Refrig 2006;29(4):539–46.

[31] Yoon SH, Kim JH, Hwang YW, Kim MS, Min K, Kim Y. Heat transfer and pressure drop characteristics during the in-tube cooling process of carbon dioxide in the supercritical region. Int J Refrig 2003;26(8):857–64.

[32] Pitla SS, Groll EA, Ramadhyani S. New correlation to predict the heat transfer coefficient during in-tube cooling of turbulent supercritical CO2. Int J Refrig 2002;25(7):887–95.

[33] Dang C, Hihara E. In-tube cooling heat transfer of supercritical carbon dioxide. Part 1. Experimental measurement. Int J Refrig 2004;27(7):736–47.

[34] Fang X. Modeling and analysis of gas coolers. United States of America: Air Conditioning and Refrigeration Center, College of Engineering, University of Illinois at Urbana-Champaign; 1999.

[35] Huai X, Koyama S, Zhao T. An experimental study of flow and heat transfer of supercritical carbon dioxide in multi-port mini channels under cooling conditions. Chem Eng Sci 2005;60(12):3337–45.

[36] Huai X, Koyama S. Heat transfer characteristics of supercritical CO_2 flow in small-channeled structures. Exp Heat Transf 2007;20(1):19–33.

[37] Pettersen J, Rieberer R, Munkejord S. Heat transfer and pressure drop characteristics of evaporating carbon dioxide in microchannel tubes. In: Proceedings of 4th IIR-Gustav Lorentzen conference on natural working fluids at Purdue; 2000. p. 107–14.
[38] Kuang G, Ohadi M, Zhao Y. Experimental study on gas cooling heat transfer for supercritical CO2 in microchannel. In: Proceedings of the second international conference on microchannels and minichannels (ICMM2004); 2004. p. 325–32.
[39] Olson DA. Heat transfer of supercritical carbon dioxide flowing in a cooled horizontal tube. (No. NIST Interagency/Internal Report (NISTIR)-6496); 2000.
[40] Koppel L, Smith J. Turbulent heat transfer in the critical region. Int Dev Heat Transf 1961:585–90.
[41] Walisch T, Dörfler W, Trepp C. Heat transfer to supercritical carbon dioxide in tubes with mixed convection. Zurich (CH): ETH Zentrum; 1997.
[42] Kuang G, Ohadi M, Zhao Y. Experimental study of miscible and immiscible oil effects on heat transfer coefficients and pressure drop in microchannel gas cooling of supercritical CO2. In: Proceedings of the ASME summer heat transfer conference. Las Vegas, NV, HT2003-47473; 2003.
[43] Dang C, Iino K, Fukuoka K, Hihara E. Effect of lubricating oil on cooling heat transfer of supercritical carbon dioxide. Int J Refrig 2007;30(4):724–31.
[44] Yun R, Hwang Y, Radermacher R. Convective gas cooling heat transfer and pressure drop characteristics of supercritical CO 2/oil mixture in a minichannel tube. Int J Heat Mass Transf 2007;50(23):4796–804.
[45] Mori K, Onishi J, Shimaoka H, Nakanishi S, Kimoto H. Cooling heat transfer characteristics of co2 and co2-oil mixtures at supercritical pressure conditions. Trans Jpn Soc Refrig Air Cond Eng 2003;20(3):407–12.
[46] Kim J, Yoon S, Kim M, Kim Y. An experimental investigation of heat transfer characteristics during in-tube gas cooling process of carbon dioxide. IIF-IIR Comm B 2001;1:17–21.
[47] Kondou C, Hrnjak P. Heat rejection from R744 flow under uniform temperature cooling in a horizontal smooth tube around the critical point. Int J Refrig 2011;34(3):719–31.
[48] Zhao C-R, Jiang P-X, Zhang Y-W. Flow and convection heat transfer characteristics of CO 2 mixed with lubricating oil at super-critical pressures in small tube during cooling. Int J Refrig 2011;34(1):29–39.
[49] Gao L, Honda T. Experiments on heat transfer characteristics of heat exchanger for CO2 heat pump system. In: Proceedings of the Asian conference on refrigeration and air conditioning. Kobe, Japan; 2002.
[50] Zingerli A, Groll E. Influence of refrigeration oil on the heat transfer and pressure drop of supercritical CO_2 during in-tube cooling. Sci Tech Froid 2001:279–89.
[51] Adebiyi G, Hall W. Experimental investigation of heat transfer to supercritical pressure carbon dioxide in a horizontal pipe. Int J Heat Mass Transf 1976;19(7):715–20.
[52] Melikpashaev N, Kobelkov V, Plyugin M. Investigation of convective heat transfer at supercritical pressures. High Temp 1968;6(2):263.
[53] Jiang P-X, Zhao C-R, Shi R-F, Chen Y, Ambrosini W. Experimental and numerical study of convection heat transfer of CO2 at super-critical pressures during cooling in small vertical tube. Int J Heat Mass Transf 2009;52(21):4748–56.
[54] Shiralkar BS, Griffith P. The deterioration in heat transfer to fluids at supercritical pressure and high heat fluxes. Cambridge, Mass: MIT Engineering Projects Laboratory; 1968. [1968].
[55] Shiralkar B, Griffith P. The effect if swirl, inlet conditions, flow direction, ail tube diameter on tie leat transfer to fluids at supercritical pressure; 1969.
[56] Baskov V, Kuraeva I, Protopopov V. Heat-transfer with turbulent-flow of a liquid at supercritical pressure in tubes under cooling conditions. High Temp 1977;15(1):81–6.
[57] Krasnoshchekov E, Protopopov V. Generalized relationship for calculation of heat-transfer to carbon-dioxide at supercritical pressure (PI = 1.02–5.25) vol. 9. 233 Spring St, New York, NY 10013-1578 USA: Maik Nauka/Interperiodica/Springer; 1971. p. 1215. [-+].
[58] Bourke P, Pulling D. An experimental explanation of deterioration in heat transfer to supercritical carbon dioxide. Atomic Energy Research Establishment; 1971.
[59] Hiroaki T, Niichi N, Masaru H, Ayao T. Forced convection heat transfer to fluid near critical point flowing in circular tube. Int J Heat Mass Transf 1971;14(6):739–50.
[60] Krasnoshchekov E, Protopopov V. Experimental study of heat exchange in carbon dioxide in the supercritical range at high temperature drops(Heat transfer in turbulent carbon dioxide pipeflow at supercritical region). High Temp 1966;4:375–82.
[61] Krasnoshchekov E, Protopopov V, Van F, Kuraeva I. Experimental investigation of heat transfer for carbon dioxide in the supercritical region. In: Proceedings of the 2nd All-Soviet union conference on heat and mass transfer. Minsk, Belarus; 1964. p. 26–35.
[62] Ikriannikov N, Petukhov B, Protopopov V. An experimental investigation of heat transfer in the single-phase near-critical region with combined forced and free convection(carbon dioxide turbulent flow heat transfer in single phase near-critical region under forced and free convection). High Temp 1972;10(1):80–3.
[63] Silin VA. Experimental investigation of deteriorated heat transfer regimes in turbulent flow of carbon dioxide of supercritical pressure (Ph.D. thesis). Moscow: Moscow Power Institute; 1973.
[64] Jackson J, Lutterodt K, Weinberg R. Experimental studies of buoyancy-influenced convective heat transfer in heated vertical tubes at pressures just above and just below the thermodynamic critical value. In: Proceedings of the joint international conference on global environment and nuclear energy system/advanced power plants; 2003, p. 15–9.
[65] Fewster J, Jackson J. Experiments on supercritical pressure convective heat transfer having relevance to SPWR. 555 North Kensington Avenue, La Grange Park, IL 60526 (United States): American Nuclear Society; 2004.
[66] Bruch A, Bontemps A, Colasson S. Experimental investigation of heat transfer of supercritical carbon dioxide flowing in a cooled vertical tube. Int J Heat Mass Transf 2009;52(11):2589–98.
[67] Liao S, Zhao T. An experimental investigation of convection heat transfer to supercritical carbon dioxide in miniature tubes. Int J Heat Mass Transf 2002;45(25):5025–34.
[68] Bae Y-Y, Kim H-Y. Convective heat transfer to CO2 at a supercritical pressure flowing vertically upward in tubes and an annular channel. Exp Therm Fluid Sci 2009;33(2):329–39.
[69] Gupta S, McGillivray D, Surendran P, Trevani L, Pioro I. Developing heat-transfer correlations for supercritical CO2 flowing in vertical bare tubes. In: Proceedings of the ICONE20-POWER2012. Anaheim, CA; July 2012.
[70] Jiang P-X, Zhang Y, Xu Y-J, Shi R-F. Experimental and numerical investigation of convection heat transfer of CO_2 at supercritical pressures in a vertical tube at low Reynolds numbers. Int J Therm Sci 2008;47(8):998–1011.
[71] Jiang P-X, Shi R-F, Xu Y-J, He S, Jackson J. Experimental investigation of flow resistance and convection heat transfer of CO 2 at supercritical pressures in a vertical porous tube. J Supercrit Fluids 2006;38(3):339–46.
[72] Bae Y-Y, Kim H-Y, Kang D-J. Forced and mixed convection heat transfer to supercritical CO 2 vertically flowing in a uniformly-heated circular tube. Exp Therm Fluid Sci 2010;34(8):1295–308.
[73] Kim H, Kim HY, Song JH, Bae YY. Heat transfer to supercritical pressure carbon dioxide flowing upward through tubes and a narrow annulus passage. Prog Nucl Energy 2008;50(2):518–25.
[74] Kim JK, Jeon HK, Lee JS. Wall temperature measurements with turbulent flow in heated vertical circular/non-circular channels of supercritical pressure carbon-dioxide. Int J Heat Mass Transf 2007;50(23):4908–11.
[75] Kurganov V, Kaptilnyi A. Flow structure and turbulent transport of a supercritical pressure fluid in a vertical heated tube under the conditions of mixed convection. Experimental data. Int J Heat Mass Transf 1993;36(13):3383–92.
[76] Fewster J. Mixed forced and free convective heat transfer to supercritical pressure fluids flowing in vertical pipes. United Kingdom: The University of Manchester; 1976.
[77] Fang X, Bullard CW, Hrnjak PS. Heat transfer and pressure drop gas coolers. ASHRAE Trans 2001;107:255.
[78] Jackson J, Hall W. Influences of buoyancy on heat transfer to fluids flowing in vertical tubes under turbulent conditions. Turbulent forced convection in channels and bundles, vol. 2, no. 1; 1979, p. 613–40.
[79] Scalabrin G, Piazza L. Analysis of forced convection heat transfer to supercritical carbon dioxide inside tubes using neural networks. Int J Heat Mass Transf 2003;46(7):1139–54.
[80] Wang J, Hihara E. Study on carbon dioxide gas cooler heat transfer process under supercritical pressures. Int J Energy Res 2002;26(14):1237–51.
[81] Kruizenga A, Li H, Anderson M, Corradini M. Supercritical carbon dioxide heat transfer in horizontal semicircular channels. J Heat Transf 2012;134(8):081802.
[82] Petrov N, Popov V. Heat-transfer and resistance of carbon-dioxide being cooled in the supercritical region. Therm Eng 1985;32(3):131–4.
[83] Lee SH, Howell JR. Turbulent developing convective heat transfer in a tube for fluids near the critical point. Int J Heat Mass Transf 1998;41(10):1205–18.
[84] Zhang XR, Yamaguchi H. Forced convection heat transfer of supercritical CO 2 in a horizontal circular tube. J Supercrit Fluids 2007;41(3):412–20.
[85] Zhou N, Krishnan A. Laminar and turbulent heat transfer in flow of supercritical CO~ 2. ASME-Publ-HTD 1995;307:53–64.
[86] Bae JH, Yoo JY, Choi H. Direct numerical simulation of turbulent supercritical flows with heat transfer. Phys Fluids 2005;17(10):105104.
[87] Petrov N, Popov V. Heat-transfer and hydraulic resistance with turbulent-flow in a tube of water at supercritical parameters of state. Therm Eng 1988;35(10):577–80.
[88] Gnielinski V. New equations for heat and mass transfer in turbulent pipe and channel flow. Int Chem Eng 1976;16(2):359–68.
[89] Kirillov P, Yur'ev Yu S, Bobkov V. Handbook of thermal-hydraulics calculations. 1990.
[90] Li H, et al. Development of a new forced convection heat transfer correlation for CO 2 in both heating and cooling modes at supercritical pressures. Int J Therm Sci 2011;50(12):2430–42.
[91] Kuang G, Ohadi M, Dessiatoun S. Semi-empirical correlation of gas cooling heat transfer of supercritical carbon dioxide in microchannels. HVAC&R Res 2008;14(6):861–70.
[92] Petukhov B. Heat transfer and friction in turbulent pipe flow with variable physical properties. Adv Heat Transf 1970;6:503–64.
[93] Filonenko G. Hydraulic resistance in pipes; 1954.
[94] Swenson H, Carver J, Kakarala Cd. Heat transfer to supercritical water in smooth-bore tubes. J Heat Transf 1965;87(4):477–83.
[95] Mokry S, Pioro I, Farah A, King K. Updated heat transfer correlations for supercritical water-cooled reactor applications; 2011.
[96] Ghajar A, Asadi A. Improved forced convective heat-transfer correlations for liquids in the near-critical region. AIAA J 1986;24(12):2030–7.
[97] Colebrook C, White C. Experiments with fluid friction in roughened pipes. Proc R Soc Lond Ser A Math Phys Sci 1937:367–81.
[98] Swanee P, Jain AK. Explicit equations for pipeflow problems. J Hydraul Div 1976;102(5).
[99] Churchill SW. Friction-factor equation spans all fluid-flow regimes. Chem Eng 1977;84(24):91–2.
[100] Ozisik MN. Heat transfer: a basic approach; 1985.
[101] Haaland SE. Simple and explicit formulas for the friction factor in turbulent pipe flow. J Fluids Eng 1983;105(1):89–90.

[102] Nikuradse J. Gesetzmäßigkeiten der turbulenten Strömung in glatten Rohren (Nachtrag). Forsch Ing 1933;4(1). [44-44].
[103] Benedict RP. Fundamentals of pipe flow. Wiley; 1980.
[104] Gupta S, Mokry S, Pioro. Developing a heat-transfer correlation for supercritical-water flowing in vertical tubes and its application in SCWRs; 2011.
[105] Bringer R, Smith J. Heat transfer in the critical region. AIChE J 1957;3(1):49–55.
[106] Shitsman M. Heat transfer to water, oxygen and carbon dioxide in near critical region. Therm Eng 1959;1:68–72.
[107] Bishop A, Sandberg R, Tong L. Forced-convection heat transfer to water at near-critical temperatures and supercritical pressures. Westinghouse Electric Corp., Pittsburgh, PA. Atomic Power Div.; 1964.
[108] Ornatsky A, Glushchenko L, Siomin E, Kalatchev S. The research of temperature conditions of small diameter parallel tubes cooled by water under supercritical pressures. In: Proceedings of the international heat transfer conference, vol. 29: Begel House Inc.; 4; 1970.
[109] Yamagata K, Nishikawa K, Hasegawa S, Fujii T, Yoshida S. Forced convective heat transfer to supercritical water flowing in tubes. Int J Heat Mass Transf 1972;15(12):2575–93.
[110] Yaskin L, Jones M, Yeroshenko V, Giarratano P, Arp V. A correlation for heat transfer to superphysical helium in turbulent flow in small channels. Cryogenics 1977;17(10):549–52.
[111] Yeroshenko V, Yaskin L. Applicability of various correlations for the prediction of turbulent heat transfer of supercritical helium. Cryogenics 1981;21(2):94–6.
[112] Kitoh K, Koshizuka S, Oka Y. Refinement of transient criteria and safety analysis for a high-temperature reactor cooled by supercritical water. Nucl Technol 2001;135(3):252–64.
[113] Domin G. Wärmeübergang in Kritischen und Berkritischen Bereichen von Wasser in Rohren. Brennst-Wäirme-Kraft 1963;15(11):527–32.
[114] Kondratev N. Heat transfer and hydraulic resistance with supercritical water flowing in tubes. Therm Eng 1969;16(8):73-＋.
[115] Gorban L, Pomet'ko R, Khryaschev O. Modeling of water heat transfer with freon of supercritical pressure vol. 19. Obninsk, Russia: ФЭИ-1766, Institute of Physics and Power Engineering (ФЭИ); 1990.
[116] Griem H. A new procedure for the prediction of forced convection heat transfer at near-and supercritical pressure. Heat Mass Transf 1996;31(5):301–5.